HHS Public Access

Author manuscript

J Neurophysiol. Author manuscript; available in PMC 2017 December 12.

Published in final edited form as:

J Neurophysiol. 2006 September ; 96(3): 1141–1157. doi:10.1152/jn.00335.2005.

Persistent Sodium Currents and Repetitive Firing in Motoneurons of the Sacrocaudal Spinal Cord of Adult Rats

P. J. Harvey, **Y. Li**, **X. Li**, and **D. J. Bennett**

Centre for Neuroscience, University of Alberta, Edmonton, Canada

Abstract

Months after sacral spinal transection in rats (chronic spinal rats), motoneurons below the injury exhibit large, low-threshold persistent inward currents (PICs), composed of persistent sodium currents (Na PICs) and persistent calcium currents (Ca PICs). Here, we studied whether motoneurons of normal adult rats also exhibited Na and Ca PICs when the spinal cord was acutely transected at the sacral level (acute spinal rats) and examined the role of the Na PIC in firing behavior. Intracellular recordings were obtained from motoneurons of acute and chronic spinal rats while the whole sacrocaudal spinal cord was maintained in vitro. Compared with chronic spinal rats, motoneurons of acute spinal rats were more difficult to activate because the input resistance was 22% lower and resting membrane potential was hyperpolarized 4.1 mV further below firing threshold (− 50.9 ± 6.2 mV). In acute spinal rats, during a slow voltage ramp, a PIC was activated subthreshold to the spike (at −57.2 ± 5.0 mV) and reached a peak current of 1.11 ± 1.21 nA. This PIC was less than one-half the size of that in chronic spinal rats (2.79 ± 0.94 nA) and usually was not large enough to produce bistable behavior (plateau potentials and self-sustained firing not present), unlike in chronic spinal rats. The PIC was composed of two components: a TTX-sensitive Na PIC (0.44 ± 0.36 nA) and a nimodipine-sensitive Ca PIC (0.78 ± 0.82 nA). Both were smaller than in chronic spinal rats (but with similar Na/Ca ratio). The presence of the Na PIC was critical for normal repetitive firing, because no detectable Na PIC was found in the few motoneurons that could not fire repetitively during a slow ramp current injection and motoneurons that had large Na PICs more readily produced repetitive firing and had lower minimum firing rates compared with neurons with small Na PICs. Furthermore, when the Na PIC was selectively blocked with riluzole, steady repetitive firing was eliminated, even though transient firing could be evoked on a rapid current step and the spike itself was unaffected. In summary, only small Ca and Na PICs occur in acute spinal motoneurons, but the Na PIC is essential for steady repetitive firing. We discuss how availability of monoamines may explain the variability in Na PICs and firing in the normal and spinal animals.

INTRODUCTION

Spinal motoneurons possess voltage-gated persistent sodium and calcium currents [persistent inward currents (PICs)] that are activated at low thresholds just above the resting membrane potential. These PICs play a major role in amplifying synaptic inputs (Deisz et al.

Address for reprint requests and other correspondence: D. J. Bennett, 513 HMRC, Univ. of Alberta, Edmonton, AB T6G 2S2, Canada (bennettd@ualberta.ca).

1991; Prather et al. 2001) and sustaining repetitive firing (Lee and Heckman 1998a,b; Schwindt and Crill 1982). PICs in motoneurons are strongly facilitated by the monoamines serotonin (5-HT: Hounsgaard and Kiehn 1989; Perrier and Hounsgaard 2003) and norepinephrine (NE: Lee and Heckman 1999), consistent with the dense monoamine innervation of motoneurons (Alvarez et al. 1998; Schroder and Skagerberg 1985). Most, but not all, 5-HT and NE in the spinal cord derives from descending brain stem tracts, and accordingly motoneurons in brain stem-intact animals (Hounsgaard et al. 1988a) and humans (Gorassini et al. 1998; Kiehn and Eken 1997) exhibit bistable behaviors consistent with large PICs. That is, PICs are large enough to produce sustained depolarizations (plateaus) and firing (self-sustained firing) that, because PICs are voltage-gated, can be turned on or off by brief excitatory or inhibitory inputs (bistable behavior). Spinal transection immediately eliminates such bistable behavior, likely because of the loss of brain stem–induced release of monoamines onto motoneurons because bistable behavior can be recovered by exogenous application of monoamines (Conway et al. 1988; Hounsgaard et al. 1988a). However, PICs are not completely eliminated by an acute spinal transection; they are usually just reduced enough to stop bistable behavior (Bennett et al. 2001).

In motoneurons of acute spinal rats, the contributions of persistent sodium currents (Na PICs) and persistent calcium currents (Ca PICs) to the total PIC have thus far not been quantified, and thus we do not know whether the loss of PICs with spinal transection mainly results from of a loss of Ca PICs, or Na PICs, or both. We do know that with long-term spinal injury (chronic spinal rat), large PICs return (Bennett et al. 2001; Li and Bennett 2003), and these include both large Na and Ca PICs of about equal size. Thus one of our objectives was to quantify the Na and Ca PICs in motoneurons of acute spinal rats and compare these to the PICs found in chronic spinal rats (Li and Bennett 2003) and other motoneurons of acutely isolated spinal cord slice preparations (motoneurons from different muscles. Turtle: Hounsgaard and Kiehn 1989; guinea pig: Hsiao et al. 1998; rat: Powers and Binder 2003). For this, we recorded PICs in motoneurons in an in vitro preparation (Bennett et al. 2001), where the sacrocaudal spinal cord was acutely removed from normal adult rats (acute spinal).

Previously, the persistent sodium current (Na PIC) has been argued to play a critical role in repetitive firing in motoneurons (Lee and Heckman 2001; Li et al. 2004a). Without a fast persistent inward current, like the Na PIC, repetitive firing is disrupted in motoneurons (Lee and Heckman 2001), as has been shown in other neurons (French et al. 1990; Urbani and Belluzzi 2000). In the course of quantifying the Na PICs in acute spinal rats, we found that, although on average the Na PIC was small, a considerable variability existed in the Na PIC amplitude: some rats had little or no Na PIC and others had moderately large Na PICs. Thus a second objective of our study was to examine how variations in the size of Na PICs affected the repetitive firing ability of motoneurons. We found that the Na PIC was absolutely essential for repetitive firing, in that the few motoneurons that lacked Na PICs also had no ability to produce steady repetitive firing even though they otherwise appeared to be healthy motoneurons with normal fast sodium spikes.

This paper forms the basis for two companion papers (Harvey et al. 2005a,b) in which we examined how monoamine receptors modulate the Na PICs in the motoneurons of this study.

There, we found that 5-HT application facilitated the Na PIC in acute spinal rats and, importantly, could rescue a cell that was initially without firing ability, by producing a Na PIC and thereby enabling repetitive firing (Harvey et al. 2005b). Furthermore, we showed that 5-HT and NE receptor antagonists could completely eliminate the Na PIC in both acute and chronic spinal rats (Harvey et al. 2005a). Thus despite the loss of brain stem–derived monoamines, spinal sources of monoamines (reviewed in Schmidt and Jordan 2000) must play a primary role in facilitating the Na PIC, and ultimately enable motoneurons to fire repetitively.

METHODS

Intracellular recordings were made from motoneurons in the in vitro sacrocaudal spinal cord of both normal adult rats (female Sprague-Dawley; 1–6 mo old, average age = 3.4 ± 1.2 mo, $n = 41$) and spastic adult rats with chronic spinal cord injury (3–5 mo old, average age = 4.0 ± 0.6 mo, $n = 34$). When the sacrocaudal cord was removed from normal rats for this in vitro recording, the cord was transected at the S_2 level at the time of removal; thus, these 41 rats were termed acute spinal rats. For the spastic chronic spinal rat, a complete spinal cord transection was made at the S_2 sacral level when the adult rat was 40–55 days old (Bennett et al. 1999, 2004). Usually, within 1 mo, dramatic spasticity developed in the tail muscles, which are innervated by sacrocaudal motoneurons below the level of the injury. Only rats >1.5 mo and <4 mo after injury, and with clear spasticity, were used for in vitro recording of the motoneurons (the 34 chronic spinal rats). Bennett et al. (1999, 2004) described the details of the chronic spinal transection and spasticity assessment. All experimental procedures were conducted in accordance with guidelines for the ethical treatment of animals issued by the Canadian Council on Animal Care, and approved by the University of Alberta Health Sciences Animal Policy and Welfare Committee.

In vitro preparation

Details of the in vitro procedures have been described in previous publications (Bennett et al. 2001; Li and Bennett 2003; Li et al. 2004b). Briefly, normal and chronic spinal rats were anesthetized with urethane (0.18 g/100 g; maximum of 0.45 g per rat for rats >250 g), and the whole caudal cord between the T_{13} and L_6 vertebrae (corresponding to spinal L_6 to cauda equina) was exposed and continuously wetted with modified artificial cerebrospinal fluid (mACSF). The rat was administered pure oxygen with a mask for 5 min before quickly removing the cord and immersing it in a dissection chamber containing mACSF. All spinal roots were removed except for the S_4 and Ca_1 ventral roots, and the dorsal surface of the cord was glued (super glue; RP 1500, Adhesive Systems) onto a small piece of nappy paper to improve stability. After a total time of 1.5 h in the dissection chamber at room temperature (20°C), the cord was transferred to a recording chamber containing normal ACSF (nACSF) maintained at 24°C and continuously flowing at >5 ml/min. The cord was secured at the bottom of the recording chamber with the ventral side up by pinning the nappy paper to which it was glued onto the Sylgard base. After allowing an hour in the recording chamber to wash out any residual anesthetic or kynurenic acid, the bathing solution was switched to nACSF containing a cocktail of fast synaptic transmission blockers (AP5, CNQX, strychnine and picrotoxin). The nACSF was oxygenated in an elevated 200-

ml source bottle and run through the recording chamber. This nACSF running out of the recording chamber was continuously collected, filtered, and returned to the source bottle using a peristaltic pump. Because of the large volume (200 ml) being recycled in this way and the small volume of the cord (<0.05 ml), a significant accumulation of metabolic byproducts was not likely.

Intracellular recording

Intracellular recording methods were as described in Li and Bennett (2003). Briefly, sharp intracellular electrodes were made from thick-walled glass capillary tubes (1.5 mm OD; Warner GC 150F-10) using a Sutter P-87 micropipette puller and filled with a mixture of 1 M K-acetate and 1 M KCl. Electrodes (Fig. 1*A*) were bevelled down from an initial resistance of 40–60 to 25–30 MΩ using a rotary beveller (Sutter BV-10). The bevel and wide electrode shaft gave good current-passing capabilities, and the sharp tip of the bevel was critical for breaking through the tough pia and connective tissue in these adult rats, before penetrating the motoneurons. A stepper-motor micromanipulator (660, Kopf) was used to advance the electrodes through the tissue and into cells. Motoneurons were identified through antidromic stimulation of the S_4 and Ca_1 ventral roots, which were wrapped around Ag·AgCl electrodes above the recording chamber and sealed with high-vacuum grease. Only motoneurons with a stable penetration, resting potential below −60 mV, and antidromic spike height >60 mV from rest were included in this study. Data were collected with an Axoclamp 2b intracellular amplifier (Axon Instruments, Burlingame, CA) running in discontinuous current clamp (DCC, switching rate 5–8 kHz, output bandwidth 5.0 kHz) or discontinuous single-electrode voltage clamp (SEVC; gain 0.8 to 2.5 nA/ mV) modes.

Drugs and solutions

Two kinds of ACSF were used in these experiments: mACSF, designed to minimize potential excitotoxicity, was used in the dissection chamber before recording, and nACSF in the recording chamber. Composition of the mACSF was (in mM) 118 NaCl, 24 $NaHCO_3$, 1.5 $CaCl_2$, 3 KCl, 5 $MgCl_2$, 1.4 NaH_2PO_4, 1.3 $MgSO_4$, 25 D-glucose, and 1 kynurenic acid. nACSF was composed of (in mM) 122 NaCl, 24 $NaHCO_3$, 2.5 $CaCl_2$, 3 KCl, 1 $MgCl_2$, and 12 D-glucose. Both types of ACSF were saturated with 95% O_2-5% CO_2 and maintained at pH 7.4. A synaptic transmission blocking cocktail was usually added to the nACSF; it consisted of 50 μM D(−)-2-amino-5-phosphonopentanoic acid (AP5; Tocris), 10 μM 6-cyano-7-nitroquinoxaline-2,3-dione (CNQX; Tocris), 1 μM strychnine (Sigma), and 100 μM picrotoxin (Tocris) to block *N*-methyl-D-aspartate (NMDA), AMPA, glycine, and $GABA_A$ receptors, respectively. Additional drugs were added as required, including 0.5–2 μM TTX (Alamone Labs) to block voltage-gated Na channels, 15 μM nimodipine (Tocris) or 400 μM Cd^{2+} (Sigma) to block voltage-gated L-type Ca channels, and 20 μM riluzole (Tocris) to block persistent sodium currents.

Persistent inward currents in current- and voltage-clamp recording

Slow triangular current ramps (0.4 nA/s) were applied to the motoneurons to measure firing and basic cell properties (Fig. 1*B*). The input resistance was measured during the ramp over a 5-mV range near rest and subthreshold to PIC onset. The firing level, or spike voltage threshold (V_{th}), was averaged from five consecutive spikes starting with the second spike on

the up ramp, and was taken as the potential at which the rate of change of membrane potential (dV/dt) first exceeded 10 V/s (Li et al. 2004a). The spike overshoot (>0 mV) was calculated as the average peak depolarization during the action potential from these same five spikes. Bistable behavior was quantified by measuring self-sustained firing (ΔI): that is, when the motoneuron continued to fire at less current than was initially required to recruit firing. This was quantified during current ramps by subtracting the current at derecruitment (I_{end}) from the current at recruitment (I_{start}), so that $\Delta I = I_{start} - I_{end}$. A subthreshold activation of the PIC (e.g., subthreshold plateau) was identified by extrapolating to higher potentials the linear subthreshold current-voltage relation (Fig. 1*B*, thin line) from a region ≥5 mV below spike voltage threshold and comparing this to the actual depolarization. In motoneurons with large PICs, the plateau potential was seen as a subthreshold acceleration (Fig. 1*B*, arrowhead) in membrane potential before the first spike, and a long after-depolarization after cessation of firing (Fig. 1*B*, double arrow). Instantaneous firing frequency (F) as a function of current (F–I relation) was computed using a custom Linux-based program (G.R. Detillieux, Winnipeg, Canada) from the current ramp recordings (Fig. 1*C*). The F–I slope was calculated for linear regions of the F–I relation using a regression. Minimum firing rate was determined by taking the average of the last interspike interval from two to three consecutive current ramps or from threshold current steps in the case of motoneurons that did not fire during normal slow current ramps. Antidromic spike height was measured after stimulation of the ventral roots while the cell was at rest.

Slow triangular voltage ramps (3.5 mV/s), from approximately −80 to −40 mV and back to −80 mV, were used to quantify the PICs (Fig. 1*D*). During the increasing portion of the ramp, the current initially increased linearly with voltage because of the passive leak conductance. A linear relation was fit in this region (10 mV below the PIC onset) and extrapolated into more depolarized potentials (Fig. 1*D*, thin line labeled leak current). With further depolarization, there was a downward deviation from this extrapolated leak current, as the PIC was activated (at V_{START}). The PIC was quantified as the peak amplitude of this downward deviation (initial peak on up ramp; Fig. 1*D*, downward arrow). Large PICs caused an outright negative slope in the current response [Fig. 1*E*; negative-slope region (NSR) in the I–V relation]. Smaller PICs produced a downward deflection in the current response (flattening of I–V slope) without producing a NSR (as in Fig. 2*B*). A linear current response, not deviating downward from the leak current line (linear I–V relation), was taken to indicate the absence of any PIC (as in Fig. 5*B*). The onset voltage of the PIC, V_{START}, was defined as the voltage at which the slope of the I–V relation was reduced to halfway from the leak current slope (maximum slope) to the minimum positive slopes (halfway to 0 in the case of cells with a NSR). This is different from the onset voltage that we previously defined for the PIC, V_{on}, which was simply the voltage at which the I–V slope first reached zero (Li and Bennett 2003). However, V_{on} is not possible to pick in cells without an NSR. Thus we do not use V_{on}.

Data analysis

Data were analyzed in Clampfit 8.0 (Axon Instruments), and figures were made in Sigmaplot 8.0 (Jandel Scientific). Data are shown as mean ± SD. A Student's t-test was used to test for statistical differences, with a significance level of $P < 0.05$.

RESULTS

Resting membrane potential of motoneurons in acute spinal rats is more hyperpolarized relative to the firing threshold than in chronic spinal rats

The whole sacrocaudal spinal cord was removed from 41 normal adult rats (1–6 mo old) and maintained in vitro. Because the cord was transected at the time of removal, this was termed the acute spinal condition. Sharp intracellular recordings were made from a total of 58 motoneurons in these acute spinal rats. These motoneurons were compared with a further 42 motoneurons that were likewise recorded in vitro, but their cords were taken from 34 rats that had undergone a sacral spinal cord transection over 1.5 mo previously (chronic spinal condition). In control motoneurons recorded before application of TTX or nimodipine, the average resting membrane potential (V_m) was about 2 mV more hyperpolarized in acute spinal rats (−72.7 ± 5.8 mV; $n = 28$) than in chronic spinal rats (−70.6 ± 7.2 mV; $n = 20$), although this was not significant because of the large variability between cells. Likewise, the average spike voltage threshold (V_{th}) was about 2 mV more depolarized in acute spinal rats (V_{th} = −50.9 ± 6.2 mV) than in chronic spinal rats (V_{th} = −52.9 ± 7.4 mV, measured during current ramp as in Fig. 1*B*), although again this was not significant. However, the difference $V_{th} - V_m$ was significantly larger in acute spinal rats (21.6 ± 5.9 mV) than in chronic spinal rats (17.4 ± 6.2 mV). Thus motoneurons in acute spinal rats rested further from threshold (hyperpolarized by about 4 mV) than in chronic spinal rats.

The membrane input resistance (R_m), measured near rest, was also significantly lower in acute spinal (5.2 ± 2.3 MΩ) compared with chronic spinal (6.7 ± 2.9 MΩ) rat motoneurons. During current ramps, acute spinal rat motoneurons required significantly more current to fire (3.7 ± 2.5 nA) compared with chronic spinal rat motoneurons (1.8 ±1.2 nA), consistent with the lower input resistance and higher spike threshold relative to rest ($V_{th} - V_m$) in acute spinal rats. Thus motoneurons in acute spinal rats were more difficult to activate than in chronic spinal rats.

The spike height and overshoot (absolute value over 0 mV), as measured during current ramps, were not significantly different in acute and chronic spinal rats (92.0 ± 8.7 and 19.3 ± 7.3 mV, respectively, in acute spinal rats vs. 88.3 ± 10.5 and 17.7 ± 7.3 mV in chronic spinal rats).

Normal motoneurons have small, but variable, PICs after acute spinal transection

When a slow voltage ramp was applied to a motoneuron in the acute spinal rat, the recorded current increased relatively linearly in the subthreshold region near rest, because of the passive leak current (Fig. 2*B*, thin line), but at more depolarized levels between −60 and −45 mV, the current usually deviated downward from the linearly extrapolated leak current (Fig. 2*B*, downward arrow from thin line). This downward deviation from the leak current was used as an estimate of the net PIC. For acute spinal rats, this PIC was 1.11 ± 1.21 nA (n = 28; Fig. 3*C*), which was significantly smaller than the net PIC for chronic spinal rats (2.79 ± 0.94 nA, $n = 7$; Fig. 3*C*; PIC measured in all cases at its peak on the upward current ramp, at downward arrow in Fig. 2, *B, D*, and *F*). The average onset voltage, V_{START}, for the acute spinal rats was −57.2 ± 5.0 mV (Fig. 3*B*).

Among acute spinal rat motoneurons, the amplitude of the PIC was highly variable. Some motoneurons (25.0%, $n = 7/28$) had small PICs that only produced an inflection in the current response, lowering the slope, but not producing an NSR (Fig. 2*B*). A further 28.6% ($n = 8/28$) of motoneurons did not exhibit detectable PICs at all, in that the current response was linear (data not shown, but see Fig. 5*B*). Finally, the remaining motoneurons (46.4%, $n = 13/28$), had PICs large enough to produce an NSR in the current response (Fig. 2*D*), although the depth of this NSR of these 13 cells was usually small (0.84 ± 0.63 nA) and significantly smaller than in a comparable population of motoneurons from chronic spinal rats (1.70 ± 0.55 nA; Fig. 2*F*). Usually, the PIC amplitudes from all motoneurons of a given rat were similar, and the above variability was caused by large between-rat variations (see DISCUSSION).

Consistent with the small PICs in motoneurons of acute spinal rats, they also had little or no self-sustained firing (ΔI small; see METHODS). That is, the ΔI in acute spinal rats was 0.16 ± 0.44 nA, which was significantly smaller than in chronic spinal rats ($\Delta I = 0.57 \pm 0.42$ nA; Fig. 2*E*) and not significantly different from zero, consistent with previous reports of bistable behavior being minimal in acute spinal rats (Bennett et al. 2001; Li et al. 2004a). Furthermore, in acute spinal rats, the firing frequency varied relatively linearly with current (Fig. 2*C*), in contrast to chronic spinal rats where there was at times an abrupt acceleration in firing (nonlinearity; Fig. 2*E*, double arrow) that has previously been shown to be caused by the onset of a large Ca PIC (Li et al. 2004a).

Although ΔI was generally low in acute spinal rats, an NSR in the total PIC was linked to self-sustained firing. Of the motoneurons that had an NSR, 11/13 exhibited some small degree of self-sustained firing, with an average $\Delta I = 0.34 \pm 0.40$ nA. For the seven cells with a PIC but no NSR, however, there was, on average, no significant self-sustained firing (average $\Delta I = 0.00 \pm 0.27$ nA). Finally, the cells that did not exhibit appreciable PICs never had self-sustained firing ($n = 8/8$); indeed, repetitive firing did not usually occur at all in these cells (see Fig. 5*A*).

Persistent sodium and calcium currents make up the total PIC in acute spinal rats

The PICs in motoneurons of acute spinal rats resulted from two major currents: a TTX-sensitive Na PIC and a nimodipine-sensitive persistent Ca PIC (mediated by nimodipine-sensitive L-type calcium channels). That is, TTX (2 μM) reduced the PIC significantly by 40.8 ± 10.1% ($n = 7$; Fig. 3*A*), suggesting that nearly one-half the PIC was caused by Na PICs. This TTX-sensitive current was directly measured by subtracting the current response before and after TTX as shown in Fig. 3*B* (trace labeled Na PIC); it was 0.44 ± 0.36 nA and had an onset voltage of −61.3 ± 3.6 mV (V_{START} in Fig. 3, *A* and *B*). The remaining PIC in TTX was quantified by subtracting the leak current (see METHODS; Fig. 3*B*, middle trace, labeled Ca PIC). This remaining TTX-resistant PIC was 0.78 ± 0.82 nA (or 59.2% of the total PIC), had an onset voltage of −54.5 ± 3.6 mV, and was mediated by calcium currents (Ca PIC) because it was blocked by the nonspecific calcium channel blocker cadmium (400 μM, $n = 4$), as in chronic spinal rat motoneurons (Li and Bennett 2003). Nimodipine (15 μM) and TTX (2 μM) also completely blocked the PIC ($n = 7$), so the Ca PIC was mediated by the nimodipine-sensitive L-type calcium channel [likely by the low-threshold CaV(1.3)

L-type Ca channel, Xu and Lipscombe 2001]. Thus as in motoneurons of chronic spinal rats (Li and Bennett 2003), the PIC in acute spinal rat motoneurons consists of only two major currents, a Na PIC and Ca PIC, both of which were initiated subthreshold to spike threshold (−50.9 mV).

The reduction of the PIC by 2 μM TTX (as in Fig. 3) was rapid and occurred just before the block of all fast sodium-spiking ability in the motoneuron (at about 2 min after application), supporting the idea that the main action of TTX on the PIC was to directly block the sodium channels underlying the Na PIC in the motoneuron. TTX also blocks any spike-mediated transmitter release onto motoneurons, and thus may possibly have indirect effects on the Ca PIC, if the Ca PIC depends on this transmitter release (e.g., 5-HT release). However, this indirect effect should be slow, because of the slow actions of such neuromodulators on the Na PIC (>10 min; Harvey et al. 2005a,b) and is thus unlikely to have affected the above results, considering the rapid action of TTX. Furthermore, as detailed below, the Ca and Na PICs do not depend on neuronal activity in the spinal cord in general, because they persist for many hours with all fast synaptic transmission blocked with CNQX, AP5, strychnine, and picrotoxin (without TTX; see METHODS). Thus we interpret the TTX-sensitive PIC as a Na PIC on the motoneuron, as shown previously in chronic spinal rats (Li and Bennett 2003).

The Na PIC was also measured by first applying nimodipine (15 μM) to block the Ca PIC (Fig. 4*A*). The remaining PIC in nimodipine was purely a Na PIC (seen after leak current subtraction in Fig. 4*B*), because it was quickly and completely blocked by 2 μM TTX (nimodipine + TTX traces in Fig. 4, *A* and *B*). The motoneuron in Fig. 4, *A* and *B*, had a particularly large PIC and clearly shows the PIC components. Figure 4, *C* and *D*, shows a motoneuron with a PIC more typical of acute spinal rats. On average, the Na PIC measured in nimodipine was 0.55 ± 0.74 nA (n = 31 motoneurons), and its onset voltage (V_{START} = −62.3 ± 6.2 mV) was significantly lower than the spike threshold (V_{th} = −50.9 ± 6.2 mV). This Na PIC was 49.5% of the total PIC measured without nimodipine (1.11 ± 1.21 nA, n = 28). Thus the Ca PIC blocked by nimodipine was, on average, 50.5% of the total PIC. This is close to the proportion of the PIC eliminated by a complete calcium channel block with cadmium (400 μM; 69.7 ± 12.8%; significant reduction; n = 3) and the proportion remaining after addition of TTX (59.2%), suggesting again that the Ca PIC is mediated by nimodipine-sensitive L-type calcium channels. Comparing across all cells in acute spinal rats, the Na PIC (peak Na PIC measured on upward ramp, as usual) was not significantly correlated with the input conductance measured at rest (correlation coefficient r = 0.06, n = 31, P = 0.7).

Using nimodipine to isolate and quantify the Na PIC is particularly convenient for several reasons: *1*) the PIC measured in nimodipine was clearly blocked by TTX and very similar to the TTX-sensitive current measured before nimodipine application in other cells (0.55 ± 0.74 nA compared with 0.44 ± 0.36 nA; Figs. 4*B* vs. 3*B*); *2*) fast sodium spikes were not affected by nimodipine (see Li et al. 2004a) and thus the relation between the Na PIC and firing could be studied; and *3*) multiple motoneuron recordings and Na PIC estimates could be obtained in the same preparation, unlike with estimating the Na PIC by direct TTX application, where no further motoneurons could be located and identified in TTX, because the antidromic ventral root activation of the motoneurons was irreversibly blocked. Thus the

nimodipine-resistant PIC was used as the standard method of quantifying the Na PIC in this and in our companion papers (Harvey et al. 2005a,b).

In nimodipine, the majority of motoneurons (58.8%; $n = 20/34$) had a small Na PIC that was not large enough to produce an NSR in the current trace, but instead only produced a flattening or inflection, as in Fig. 5*D*. A few motoneurons had a large enough Na PIC to produce an NSR (11.8%; $n = 4/34$), as in Fig. 5*F*. The remaining cells (29.4%, 10/34) exhibited no detectable Na PIC, with a relatively linear *I–V* relation, as in Fig. 5*B*.

Na PIC and Ca PIC are both much larger after chronic injury

The sodium and calcium components of the PIC in motoneurons of chronic spinal rats were much larger than those measured in acute spinal rats. Consistent with our earlier observations (Li and Bennett 2003), the total PIC in chronic spinal rat motoneurons was 2.79 ± 0.94 nA ($n = 7$ cells before TTX application; see Fig. 3*C* and large PIC in Fig. 2*F*), and this was reduced in TTX by 0.97 ± 0.46 nA (34.8%; TTX-sensitive Na PIC), leaving a 1.82 ± 0.78 nA calcium PIC (65.2% of total) that was nimodipine-sensitive. Likewise, when nimodipine was added alone to motoneurons of chronic spinal rats, the remaining PIC (Na PIC estimate in nimodipine) was 1.31 ± 0.93 nA ($n = 19$), which was similar to the Na PIC measured by direct application of TTX (0.97 ± 0.46 nA). Either method of estimating the Na and Ca PICs gave currents in chronic spinal rats that were more than double those in acute spinal rat motoneurons (Na PIC 220–238%, and Ca PIC 233–264% of the values in acute spinal rat motoneurons, both differences significant; Fig. 3*C*). These large PICs almost always produced NSRs in the *I–V* relation ($n = 17/20$), as in Fig. 2*F*, and as previously reported (Li and Bennett 2003). In chronic spinal rats, the onset voltage (V_{START}) of the Na and Ca PICs were, respectively, −65.3 ± 6.3 and −57.1 ± 7.1 mV, which were a few millivolts lower, although not significantly different, than the corresponding V_{START} values in acute spinal rats. The Na PIC onset (V_{START}) was significantly lower than the spike voltage threshold (V_{th}), as in acute spinal rats. In summary, after chronic spinal injury, the PICs were twice as large as those seen in acute spinal injury, but were still made up of Na and Ca PICs in similar proportions (about 40% Na PIC and 60% Ca PIC) and with similar onset voltages. Across all motoneurons of chronic spinal rats, the Na PIC was weakly, but significantly, correlated with the input conductance (correlation coefficient $r = 0.47$, $n = 19$, $P = 0.04$).

PICs do not require fast synaptic transmission or spike-mediated transmission

With the exception of some motoneurons to which we initially added TTX or Cd^{2+} (e.g., Fig. 3), all the results described in this paper were recorded during a complete blockade of fast synaptic transmission using CNQX, AP5, strychnine, and picrotoxin to block the AMPA/kainate, NMDA, glycine, and $GABA_A$ receptors, respectively (see METHODS). Under this condition, the total PIC was not significantly different to the total PIC previously reported without this synaptic blockade (Li and Bennett 2003). Thus the total PIC did not depend on fast synaptic transmission (such as NMDA receptor activation) or associated spinal circuit behavior. Also, in fast synaptic blockade, large Ca and Na PICs existed in motoneurons of chronic spinal rats (see Fig. 2*F*), as seen without this blockade (Li and Bennett 2003). However, there was a tendency (although not quite significant, $P = 0.09$) for

there to be relatively smaller Na PICs in the fast synaptic blockade compared with without (Na PIC was 29.6 ± 5.2% of total PIC in synaptic blockade compared with 39.5 ± 12.0% without). Thus blockade of fast synaptic transmission may have indirectly eliminated a neuromodulator that somewhat facilitated the Na PIC, and at the same time inhibited the Ca PIC, so that there was no net effect on the total PIC. Interestingly, $GABA_B$ receptor activation has this effect on motoneurons (Li et al. 2004c), and thus there may have been tonic GABAergic neuron activity that was blocked by the fast synaptic blockade.

In general, we found that the fast synaptic transmission blockade rendered the cord electrically completely silent, with no spontaneous synaptic potentials or synaptic noise recorded on the motoneurons (data not shown). Thus if transmitters endogenous to the spinal cord (e.g., 5-HT in cut descending terminals or intrinsic 5-HT neurons) were in part responsible for enabling the large PICs that we recorded with fast synaptic blockade (see DISCUSSION and Harvey et al. 2005a), these neuromodulatory transmitters must have been released from last-order neurons (not depending on excitation) directly onto the motoneurons. This transmitter (e.g., 5-HT) may have been released from these last-order neurons in a manner that does not depend on spiking (leak through spontaneous vesicle release) because the Ca PIC persisted for hours (≤5 h tested) when recorded in the presence of TTX (which blocks spike transmission and Na PIC, $n = 6$).

Motoneurons that lack Na PICs show poor repetitive firing

The large variation in Na PICs in acute spinal rats provided an opportunity to examine the role of the Na PIC in recruitment and firing of motoneurons. In the few motoneurons that entirely lacked Na PICs (Fig. 5*B*; $n = 10/34$), repetitive firing was difficult to initiate, as would be predicted given the importance of Na PICs in firing (see riluzole experiments described below; and Lee and Heckman 2001; Li et al. 2004a). That is, during our standard slow current ramp, firing was not usually initiated in these neurons (80% of these neurons had no firing, $n = 8/10$ neurons); instead, the response was simply a linear depolarization of the membrane potential, even when the potential increased well past the average spike threshold (−50.9 ± 6.2 mV), up to −40 mV (Fig. 5*A*). In one-half of these neurons, faster ramps could sometimes initiate high-frequency firing (50%; $n = 4/8$ neurons; data not shown), but the remaining neurons ($n = 4/8$) could not fire repetitively at all during ramps (Fig. 5*A*), even during fast current ramps ≤4 nA/s (10 times normal slow ramp speed). The latter motoneurons, with no steady repetitive firing ability during fast ramps, were able to fire transiently but only during antidromic activation (Fig. 5*A*, *inset*) or fast current steps (Fig. 6, *A* and *B*). Usually, prolonged step depolarizations would only generate a few spikes at the leading edge of the step (Fig. 6*A*). Occasionally, during very large current steps, these neurons could fire repetitively throughout the step, but only at high rates well above the usual minimum rate in acute motoneurons (≫6 Hz; Fig. 6*B*).

The neurons that lacked Na PICs ($n = 10/34$) were not damaged cells in that they exhibited a healthy resting potential (average $V_m = -72.6 \pm 4.7$ mV) and input resistance (average $R_m = 3.5 \pm 1.2$ MΩ). More importantly, they also had large healthy fast sodium spikes (average spike height was 84.3 ± 12.7 mV) that could be evoked by antidromic stimulation (Fig. 5*A*, *inset*) or current steps (Fig. 6*A*). Thus the poor spike initiation and repetitive firing in these

cells was not caused by a direct failure of the fast sodium spike. Also, based on their input resistance, antidromic stimulation response latency, spike shape (data not shown), and long afterhypolarization (AHP; Fig. 5*A*, *inset*), these recordings were definitely from motoneurons proper and not from motor axons. When some firing was evoked in these motoneurons without a Na PIC (e.g., with a fast ramp), maximum rate of rise of potential during the first spike of repetitive firing (dV/dt_{max}) was significantly less in these neurons (126.8 ± 41.4 V/s) than in motoneurons that had a Na PIC (163.6 ± 28.1 V/s). This might, in part, simply be the lack of a Na PIC that accelerates the membrane potential before the spike, but also may reflect greater fast transient sodium channel inactivation, as has previously been suggested in other motoneurons with spike accommodation (Schlue et al. 1974). Perhaps the amount of fast sodium channel inactivation and the size of the Na PIC are linked, if a common sodium channel underlies both transient and persistent sodium currents (Crill 1996).

Recruitment and firing occurs in acute spinal neurons with small Na PICs

In contrast to motoneurons without Na PICs, motoneurons that had even small Na PICs were readily recruited and fired repetitively during slow current ramps (Fig. 5*C*, in nimodipine). Typically, motoneurons in acute spinal rats had small Na PICs that were not large enough to produce an NSR in the *I–V* relation, as described above (Fig. 5*D*; $n = 20/34$), and thus could not exhibit bistable behavior (e.g., plateaus, self-sustained firing, or after-potentials). However, the Na PIC produced a downward (inward) inflection in the *I–V* relation, and this always occurred subthreshold to the firing level ($V_{START} < V_{th}$); thus the Na PIC was able to assist in recruiting the neuron. That is, during slowly increasing current ramps, the Na PIC activation caused an acceleration in the depolarization just subthreshold to firing. This subthreshold acceleration was caused by the Na PIC, because it was blocked by TTX (see Fig. 10*D*), and it did not occur in cells that did not have a Na PIC, even when a fast ramp was used to induce firing (data not shown). Furthermore, motoneurons without a Na PIC did not fire during slow ramps, as described above, and thus it is this Na PIC-mediated subthreshold acceleration that is critical for initiating spiking with normal speed current ramps (see DISCUSSION). In some neurons with clear Na PICs, this subthreshold acceleration was accompanied by a small oscillation in the membrane potential (noise) just before recruitment (about 2-mV oscillations at about 10 Hz; e.g., *left* of *inset* in Fig. 7*B*; also see Fig. 6*A* in Li et al. 2004a), and this oscillation was also mediated by sodium currents (e.g., Na PIC, as in Geijo-Barrientos and Pastore 1995) because it was not seen in TTX. In these cells, the first spike at recruitment was triggered by one of these noisy oscillation cycles.

In most motoneurons of acute spinal rats with typical small Na PICs (not large enough to produce an NSR) after recruitment, the firing continued at currents above the recruitment threshold, but, as soon as the injected current dropped below recruitment threshold (during the downward current ramp), firing stopped and the potential decreased symmetrically to the response on the upward ramp (no after-potential; Fig. 5*C*, in nimodipine). These cells showed no self-sustained firing during slow current ramps (ΔI never more than 0; Fig. 5*C*) and at times exhibited some late spike frequency adaptation, with $\Delta I < 0$ (data not shown), unlike in chronic spinal rats (Li et al. 2004a) or in acute spinal rats with NSRs induced by a large Na PIC (Fig. 5*E*).

In these neurons without a large enough Na PIC to produce an NSR, the average minimum firing rate was 8.3 ±3.1 Hz, and the corresponding interspike interval was 120 ± 45 ms, which was similar to the AHP duration (50–150 ms; Fig. 6, *B* and *C*; see also Li et al. 2004a). Importantly, these neurons never produced steady very slow firing (<6 Hz) as described below for neurons with an NSR. Thus a Na PIC–induced NSR is critical for steady slow firing at <6 Hz.

Motoneurons with an NSR had enhanced firing

A few motoneurons of acute spinal rats ($n = 4/34$) exhibited such large spontaneous Na PICs (measured in nimodipine; Fig. 5*F*) that they had a large NSR in the current-voltage relation, which theoretically indicated that these cells should exhibit all-or-nothing bistable behavior (sodium plateau potentials and self-sustained firing), as is common in motoneurons of chronic spinal rats (Li et al. 2004a). Indeed, these large Na PICs were associated with self-sustained firing during triangular current ramps ($\Delta I > 0$; Fig. 5*E*) or after pulses (Fig. 7*B*). Also, these motoneurons with large Na PICs had subthreshold sodium plateau potentials that led to a large acceleration in potential before recruitment (Fig. 5*E*, arrowhead), and an after-potential after derecruitment (double arrow). Ultimately, the response to the triangular current ramp was asymmetrical, with more firing on the downward ramp and a prolonged depolarization (after potential), unlike in other acute spinal rat motoneurons. The subthreshold acceleration before recruitment was caused by the Na PIC, because it was blocked by TTX (data not shown), as described above for cells with smaller Na PICs, and clearly led to the initiation of the first spike during a current ramp.

Large Na PICs allow very slow steady firing

These few extreme motoneurons in acute spinal rats with large enough Na PICs to produce an NSR all produced very slow firing (<6 Hz, corresponding to interspike intervals much longer than the AHP duration) when the membrane potential was near threshold (Figs. 6*D* and 7*B*); this, too, relied on the bistable (plateau) behavior of the Na PIC. On average, the minimum firing rate in these four cells (5.0 ± 0.8 Hz) was significantly lower than the average minimum rate in motoneurons of acute spinal rats without NSRs (8.3 ± 3.1 Hz) and closer to that in chronic spinal rats (4.6 ±1.9 Hz, in nimodipine).

Previously, Li et al. (2004a) showed that chronic spinal rat motoneurons with large Na PICs exhibit similar very low frequency steady firing (very slow firing, much <6 Hz) with interspike intervals ≤1 s and much longer than the AHP duration (50–150 ms). This very slow firing depends on the Na PIC (eliminated by a Na PIC block) but not the Ca PIC (nimodipine-resistant, Li et al. 2004a). We also found that motoneurons of chronic spinal rats exhibited very slow firing (in nimodipine); furthermore, we found that this very slow firing persisted in the presence of fast synaptic transmission blocking agents (including AP-5) and thus does not depend on persistent calcium currents or NMDA receptors (Fig. 7*A*).

The detailed mechanism of how the Na PIC causes very slow firing is shown in Fig. 7 for both chronic and acute spinal rats (see also Li et al. 2004a). When the membrane potential was just subthreshold for the spike, the Na PIC came on slowly, causing an initially slowly

increasing subthreshold sodium plateau (see slow ramp-up in potential at vertical arrow in Fig. 7*A*). Furthermore, as the potential depolarized during this plateau, the Na PIC came on much more quickly (Na PIC is a fast current at more depolarized levels; Li and Bennett 2003), and thus helped accelerate the potential just before the spike (at arrowheads), and ultimately helped initiate a spike (*left* of *inset* in Fig. 7, *A* and *B*). However, because the Na PIC deactivates quickly with hyperpolarization (Li and Bennett 2003), the spike's AHP deactivated the Na PICs/plateau (potential well below V_{START} of Na PIC, thin line) and left the membrane potential again just subthreshold for the spike at the end of the 100-ms AHP (AHP estimated from antidromic pulse at rest, indicated with bar). The sodium plateau then reactivated (bracketed by thick arrows) and produced a second spike, but again this plateau was terminated by the AHP. This repeated sodium plateau (Na PIC) activation and deactivation behavior caused slow firing, because this slow firing was eliminated with a low dose of TTX (0.5 μM) or riluzole (20 μM) that reduced the Na PIC and eliminated the NSR before blocking spiking (data not shown, but see Li et al. 2004a).

Considering the dependence of slow firing on the Na PIC, the larger Na PICs in chronic spinal rat motoneurons should explain the higher incidence of slow firing compared with that of acute spinal rats; furthermore, cells with larger Na PICs ought to, in general, have lower minimum rates. To examine this, we determined the relationship between the minimum firing rate and the Na PIC amplitude (Fig. 8*A*). For chronic spinal rat motoneurons, there was indeed a significant correlation between Na PIC amplitude and the minimum firing rate (●, thick regression line; $r = 0.538$, $n = 19$, $P = 0.02$), and most of these motoneurons had an NSR (Fig. 8*B*, ●). Furthermore, cells with Na PICs >1.3 nA (mean Na PIC amplitude) had a much lower minimum firing rate (3.3 ±1.2 Hz, $n = 7$) compared with the minimum rate in cells with Na PICs <1.3 nA (5.4 ±1.8 Hz; $n = 12$; significant difference). Acute spinal rat motoneurons exhibited a trend toward this relationship, but the correlation was not quite significant (○, thin regression line; $r = 0.302$, $n = 25$, $P = 0.1$) because there were only a few neurons with a large Na PIC. However, the four cells that did have a large enough Na PIC to produce a clear NSR (○ at *right* of Fig. 8*B*) exhibited some of the slowest firing among this group of cells (<6 Hz, significantly lower rate than cells without an NSR). Thus larger persistent sodium currents, especially those that induced NSRs, are associated with lower minimum firing rates.

Frequency-current slope is not related to Na PIC amplitude

When only a Na PIC was present (with Ca PIC blocked with nimodipine), during increasing current ramps, the firing rate response increased relatively linearly (linear *F–I* relation; Fig. 5*E*). As previously reported (Li et al. 2004a), this is because the Ca PIC causes the main nonlinearity in the *F–I* relation (acceleration in firing; Fig. 2*E*, *top*, double arrow), and this nonlinearity is blocked by nimodipine. On average, the slope of the *F–I* relation in nimodipine was significantly smaller in chronic spinal rats (5.5 ±1.6 Hz/nA; $n = 16$) compared with in acute spinal rats (7.4 ± 2.3 Hz/nA; $n = 16$; Fig. 9, *right*). Because the chronic spinal rats have larger Na PICs, this might suggest that a shallower *F–I* slope is associated with larger Na PICs. However, the *F–I* slope was not significantly correlated to Na PIC amplitude in either acute or chronic spinal rat motoneurons (Fig. 9; acute: thin line, $r = 0.157$; chronic: thick line, $r = 0.138$). We also found that the *F–I* slope was not

significantly correlated with the minimum slope-conductance of the *I–V* relation, G_{min} (where G_{min} is the slope of the *I–V* relation at the NSR in cells with a NSR, or just the minimum slope in other cells; $r = 0.221$, $n = 18$, $P = 0.4$). Thus the *F–I* slope is not related to the Na PIC, unlike with the Ca PIC (Li et al. 2004a). Considering that changes in the Na PIC are not associated with changes in the *F–I* slope, whereas increases in the Na PIC lower the minimum firing rate, the major action of the Na PIC on the *F–I* relation is to vertically shift the *F–I* relation to lower rates (cf. frequency plots in Fig. 5, *C* and *E*), allowing an overall broader range of firing (maximum rate in acute and chronic spinal rats is similar, data not shown).

Na PICs are essential in firing

To definitively prove that the Na PIC was essential for steady repetitive firing, we blocked the Na PIC without blocking the spike, using either a low dose of TTX (<1 μM, $n = 6$) or riluzole (20 μM, $n = 9$, combined data from acute and chronic spinal rats). When low-dose TTX was applied to a motoneuron, the Na PIC was blocked (Fig. 10, *B* and *E*) before affecting the fast sodium spike (Fig. 10*C*), because the Na PIC is more sensitive to sodium channel blockers (Stafstrom et al. 1985). This low dose of TTX (0.5 μM; as in Fig. 10, *D–F*) gave a longer period of time where the fast sodium spike was unaffected while the Na PIC was blocked (minutes; Na PIC measured in nimodipine), compared with the normal 2-μM dose, which blocked both almost simultaneously. Riluzole (20 μM) had the same effect as low-dose TTX, but worked very slowly, taking 1 h to completely block the Na PIC (data not shown) and another hour to affect the fast sodium spike. With either TTX or riluzole, during the period when the Na PIC was blocked and the spike was unaffected, the repetitive firing during a current ramp was always eliminated (cf. firing in Fig. 10*A* to lack of firing in Fig. 10*D*). Thus the Na PIC was absolutely essential for spike initiation during a ramp. During this period, a fast current step still initiated a few spikes (Fig. 10, *C* and *G*), and this was how we showed that the fast spike was unaffected after the Na PIC block (overlapping spikes in Fig. 10*C*, before and after low-dose TTX). However, this step-evoked firing was never sustained (Fig. 10*F* in TTX and Fig. 10*G* in riluzole), and thus sustained repetitive firing also required a Na PIC. Antidromic activation of the motoneurons also initiated normal full-height sodium spikes in riluzole (Fig. 10*H*).

Repeated short intracellular current pulses (data not shown) or antidromic stimulation at moderately low frequencies (10 Hz; Fig. 10*H*) usually gave repeated full unattenuated spikes, showing that failure to fire repetitively during a ramp or step input was not simply caused by a failure of spikes with repetition. However, higher-frequency stimulation (20 Hz) at times led to spike inactivation, with a broadening of the spike over the course of many stimulations and ultimately complete failure of spiking (Fig. 10*I*, *). Such spike inactivation did not occur before riluzole or low-dose TTX (see repetitive firing in Fig. 10*A*), and thus subtle changes in the fast sodium channel inactivation occurred in addition to the block of the Na PIC with these drugs. Thus spike initiation and repetitive firing depends primarily on the Na PIC but also on a relative lack of spike inactivation.

The cells just described in Fig. 10 were recorded in the presence of nimodipine to block the Ca PIC; in these cells, there was robust repetitive firing during a current ramp (Fig. 10*A*) and

clear Na PICs (Fig. 10*B*) before the application of TTX or riluzole. In the absence of nimodipine, application of TTX or riluzole to block the Na PIC also eliminated repetitive firing during a current ramp (data not shown) before blocking the fast sodium spike. Thus the Ca PIC itself is not sufficient for steady repetitive firing. In low-dose TTX without nimodipine, there was still a Ca PIC that produced a calcium plateau in chronic spinal rats (Li et al. 2004a), and this sometimes triggered a few spikes at its onset (data not shown). In this way, the Ca PIC onset acted like a current step (as in Fig. 10, *E* and *G*), producing a rapid depolarization that initiated a spike.

DISCUSSION

The results show that normal motoneurons have Na and Ca PICs immediately after spinal transection (acute spinal condition), but these are small and only increase substantially with long-term injury (chronic spinal). Interestingly, the PICs occur immediately after spinal transection despite the massive loss of brain stem–derived monoamines (5-HT and NE) that normally regulate PICs (Hounsgaard et al. 1988a; Hultborn and Kiehn 1992; Lee and Heckman 1998a). The small PICs in acute spinal rats generally do not lead to pronounced bistable behavior (plateau potentials and self-sustained firing), consistent with previous studies of acute spinal animals (cat: Conway et al. 1988; turtle: Hounsgaard et al. 1988b; guinea pig: Nishimura et al. 1989; rat: Powers and Binder 2003). However, these PICs are usually sufficient to at least produce an inflection (flattening) in the *I–V* relation, which has previously been argued to underlie graded amplification of motoneuron responses near threshold (as in Fig. 5, see also Li and Bennett 2003; Prather et al. 2001; Schwindt and Crill 1982) and participate in recruitment and repetitive firing.

The results also show that all motoneurons that lack the ability to produce steady repetitive firing during slow current ramps also lack a Na PIC, suggesting that Na PICs are necessary for steady repetitive firing. Conversely, most neurons that did not have any detectable Na PIC could not fire repetitively during a slow current ramp. A few of these neurons could fire repetitively during slow ramps (2/10), but this may have been caused by small Na PICs that were not detectable. That is, even when an *I–V* relation is relatively linear, suggesting no detectable Na PIC (see METHODS), TTX application can at times still reveal a small TTX-sensitive Na PIC (unpublished data). Taken together, these results suggest that repetitive firing is highly correlated with the presence of a Na PIC.

To directly prove that the Na PIC is essential for repetitive firing, the Na PIC must be blocked without blocking the sodium spike, and this has been done by blocking the Na PIC with riluzole or low-dose TTX (see RESULTS), or using a depolarization block (Lee and Heckman 2001). In riluzole or low-dose TTX, repetitive firing is eliminated as expected when the Na PIC is blocked, even though transient firing is possible with a fast current step. Thus riluzole creates a situation like in neurons that naturally lack Na PICs (cf. Figs. 10*D* and 5*A*). This verifies the essential role of the Na PIC in repetitive firing, supporting the conclusions of Lee and Heckman (2001) in cat motoneurons and Stafstrom et al. (1985) in cat neocortical cells. Further evidence for the role of the Na PIC in firing comes from our companion papers, where we show that motoneurons that lack repetitive firing and Na PICs can be rescued by application of 5-HT_2 receptor agonists, which increase the Na PIC

amplitude and thus enable repetitive firing (Harvey et al. 2005b). Conversely, 5-HT and NE antagonists eliminate the Na PIC and repetitive firing, like riluzole, although these antagonists do so by indirectly modulating the Na PIC through receptors linked to Gq-protein–coupled intracellular pathways (Harvey et al. 2005a).

Variation in Na PIC amplitude with state of animal preparation

In acute spinal rats, the Na PIC is usually large enough to assist in spike initiation and enable repetitive firing, but not so large as to produce bistable plateau behavior. In a few extreme acute spinal rat motoneurons (11.8%), the Na PIC is so large that it does produce a substantial NSR in the *I–V* relation that enables Na plateaus and slow subthreshold oscillations, resulting in the characteristic very slow firing seen with large Na PICs (Li et al. 2004a). On the other extreme, in the motoneurons without clear Na PICs (29.4%), repetitive firing is poor or absent, consistent with the fundamental role of the Na PIC in enabling repetitive firing. From the wide variation in Na PICs in acute spinal rats, it is clear that any motoneuron that can produce steady repetitive firing is likely to have at least a small Na PIC, and larger Na PICs are associated with slower firing (lower minimum rates).

For comparison, it is noteworthy that motoneurons from deeply pentobarbitol-anesthetized animals have no evidence of bistable behavior (no plateaus or self-sustained firing, Lee and Heckman 2001; Powers and Binder 1995; Prather et al. 2001), consistent with a direct inhibition of the Ca PIC by pentobarbitol (Guertin and Hounsgaard 1999) and reduced brain stem activity in this preparation. However, many motoneurons in these anesthetized animals still fire repetitively during a slow current ramp or steady current step; thus given the absolutely critical role of the Na PIC in steady repetitive firing, it is likely that some weak Na PIC exists in these motoneurons. Indeed, Lee and Heckman (2001) have shown that a persistent inward current with characteristics of the Na PIC does exist in motoneurons of pentobaritol-anesthetized cats. However, it is not uncommon to encounter healthy motoneurons in anesthetized cats that will not exhibit steady repetitive firing (C. J. Heckman, unpublished data; Granit et al. 1956). These are typically not reported on in detail and considered abnormal (termed phasic or accommodating in early reports, Granit et al. 1956), but, in retrospect, they may simply be healthy motoneurons that lack a Na PIC, as we have seen.

In contrast, PICs in brain stem–intact decerebrate cats or intact rats or humans produce pronounced bistable behavior, including long-lasting self-sustained firing (Eken et al. 1989; Gorassini et al. 1998; Hounsgaard et al. 1988a; Kiehn and Eken 1997), likely because of facilitation from brain stem-derived monoamines. Thus on a continuum, PICs are smallest in the barbiturate-anesthetized state, larger in the acute spinal state, and largest in the brain stem–intact state. The latter may vary considerably depending on brain stem activity, and the brain stem–intact decerebrate cat likely does not have as large PICs as in the intact awake animal or human (Gorassini et al. 1998), because we know that PICs can be further increased in the decerebrate state by application of 5-HT or NE agonists (Conway et al. 1988; Hounsgaard et al. 1988a; Lee and Heckman 1999). The effect of PICs in chronic spinal rats (e.g., self-sustained firing) are at least as large as in normal intact animals (see Li et al. 2004a), and thus serve as a reasonable comparison to those in acute spinal rats.

Role of endogenous monoamines in regulating Na PIC and general motoneuron properties

Considering that the PICs can be very small or absent in healthy motoneurons of some acute spinal animals, the question is as follows: what enables the moderately large PICs in other acute spinal animals? We know that many exogenously applied neuromodulators, including 5-HT, NE, acetylcholine, and glutamate, can facilitate PICs in motoneurons (Alaburda and Hounsgaard 2003; Delgado-Lezama et al. 1997; Hultborn and Kiehn 1992; Kiehn and Harris-Warrick 1992; Lee and Heckman 1999). However, the results from our companion paper (Harvey et al. 2005a) suggest that Na PICs in the spinal animal depend primarily on residual monoamines (5-HT and NE) in the spinal cord (the level of these residual monoamines we refer to as monoamine tone). That is, in spinal rats, the naturally occurring Na PICs and associated repetitive firing are blocked by antagonizing monoamine receptors, and thus there must be some endogenous monoamine tone underlying these Na PICs (Harvey et al. 2005a). Furthermore, application of monoamine receptor agonists facilitates the Na PIC and rescues firing in motoneurons that otherwise cannot fire repetitively (Harvey et al. 2005b), suggesting that they initially lacked monoamine tone. In general, variations in monoamine tone may underlie the variations in PICs from rat to rat, and so rats that have little monoamine tone have little or no PICs, and do not fire slowly. The fact that motoneurons fire repetitively in reduced preparations where the spinal cord is acutely sliced (Perrier et al. 2000) or where motoneurons are cultured (Kuo et al. 2004) suggests that residual monoamines, or a similar neuromodulator, are also available to facilitate the Na PIC in these more reduced preparations, although this remains to be verified.

The origins of the monoamines in acute and chronic spinal rats are discussed in a companion paper (Harvey et al. 2005a). Suffice it to say, there are residual monoamines in the spinal cord facilitating both Na and Ca PICs, even in the chronic spinal rat (Cassam et al. 1997; Newton and Hamill 1988). Furthermore, these results indicate that these monoamines must be released from spinal sources (e.g., 5-HT neurons) that do not depend on general neuronal activity, because Ca and Na PICs persist in a blockade of fast synaptic transmission that renders the cord synaptically quiet. Whether the release of 5-HT from these cells is from spontaneous firing or from non–spike-mediated transmitter release (leak) is uncertain, although there may be some leak because Ca PICs persist in long-term blockade of spikes with TTX.

PICs in motoneurons of chronic spinal rats become supersensitive to monoamines, as to be expected from the massive denervation from the descending brain stem monoamine tracts (Harvey et al. 2005b). Thus small amounts of residual monoamines in the cord produce large PICs, and this ultimately explains the large PICs found in the chronic spinal rats (Harvey et al. 2005a). This denervation supersensitivity of PICs essentially replaces the effect of the lost brain stem monoamines, returning the motoneurons to a state closer to that of the normal intact animal. Supersensitivity to residual monoamines after chronic injury likely also explains why motoneurons of chronic spinal rats have a higher input resistance and rest closer to the spike threshold than motoneurons of acute spinal rats (see RESULTS). That is, in addition to its effects on PICs, 5-HT also increases the input resistance in motoneurons (White and Fung 1989), depolarizes the resting membrane potential (White and Fung 1989) and hyperpolarizes the spike threshold (Fedirchuk and Dai 2004; Harvey et al. 2005b). All

these membrane properties become supersensitive to 5-HT in chronic spinal rats (Harvey et al. 2005b), and thus supersensitivity to residual spinal 5-HT should increase the input resistance and depolarize cells closer to the spike threshold, as is observed in motoneurons from chronic spinal rats.

Role of Na PIC in repetitive firing

The Na PIC is always activated subthreshold to the spike, and thus plays a major role in spike initiation (see RESULTS, and Crill 1996; Li et al. 2004a). Without a Na PIC, during slowly increasing excitation to a motoneuron (ramp), the membrane potential slowly depolarizes and spikes are not initiated (as in Fig. 5*A*), likely because inactivation of the transient sodium channel overwhelms its activation (as suggested by Lee and Heckman 2001). A spike can be initiated during a more rapid depolarizing excitation (such as a step; Fig. 6*A*), because the rapid excitation replaces the action of the Na PIC. Once firing is initiated, it can continue, provided that the depolarizing upswing at the end of each AHP is rapid enough to initiate a spike without the help of large Na PICs, and this may explain why fast repetitive firing is possible in some acute spinal motoneurons that lack Na PICs (as in Fig. 6*B*) or in hypoglossal motoneurons when the Na PIC is reduced with phenetol (Zeng et al. 2005). Basically, any form of depolarization that sufficiently rapidly depolarizes the membrane (above a minimum slope dV/dt) can initiate a spike (such as a fast onset Ca PIC). However, except during rapid firing, the upswing at the end of the AHP is slow and insufficient to cause spike initiation by itself, so firing stops after a few spikes. This is the usual situation in the extreme acute spinal motoneurons that have little or no Na PIC (as in Fig. 6*A*). Furthermore, cells without a Na PIC show evidence of somewhat increased spike inactivation (see RESULTS), which makes spike initiation and firing even more difficult. This subtle spike inactivation invariably occurs when the Na PIC is blocked with riluzole (see RESULTS Fig. 10*I*) or monoamine antagonists (Harvey et al. 2005a) or when the Na PIC is just spontaneously absent (see RESULTS), consistent with the idea that different activation states of the same sodium channel may underlie the spike and the Na PIC (Alzheimer et al. 1993; Crill 1996; Taddese and Bean 2002).

Most normal motoneurons in acute spinal rats do, however, have some Na PIC, and this clearly serves to enable repetitive firing, because they fire repetitively during a steady or slowly increasing current injection (see DISCUSSION above and riluzole results). When a Na PIC is present, the spikes are initiated because the Na PIC produces a rapid depolarization (subthreshold acceleration, Fig. 5*E*) that presumably helps the activation of the spike escape its inactivation, during a slow current ramp. Furthermore, the Na PIC is known to be rapidly deactivated on hyperpolarization (unlike the Ca PIC; Li and Bennett 2003), and thus each AHP must at least partly deactivate the Na PIC (see RESULTS). Therefore after each AHP, the Na PIC is again available to activate and help initiate a new spike. In this way, the Na PIC enables repetitive firing. Just at threshold the Na PIC initially comes on slowly (ramps up), but eventually it comes on more rapidly, causing a rapid acceleration that triggers a spike (at arrowheads in Fig. 6 or 7). This slow followed by fast activation could be caused by a voltage-dependent time constant of the Na PIC (like with the Ca PIC; Li and Bennett 2003) or by two distinct Na currents making up the Na PIC: one slower sodium current and a second faster higher threshold sodium current.

As the firing rate increases, the firing level rises and the AHPs produce less absolute hyperpolarization; thus ultimately, the minimum potential reached during AHPs is more depolarized during fast firing (i.e., bottoms of AHPs depolarize; Figs. 2*E* and 5*E*; see also Schwindt and Crill 1982). Thus the Na PIC should be less affected (less deactivated) by the AHPs during fast firing. Thus the Na PIC may not play such a critical role in fast firing, which is consistent with the finding that reducing the Na PIC with monoamine antagonists does not lower the *F–I* slope (Harvey et al. 2005a) and reducing the Na PIC with phenetol does not affect late spike frequency adaptation during fast firing (Zeng et al. 2005). Furthermore, the *F–I* slope does not increase in cells with larger Na PICs (Fig. 8). Oddly enough, Lee and Heckman (2001) found a positive correlation with the *F–I* slope and Na PIC. However, they only indirectly inferred the Na PIC from the response to high-frequency oscillations (120 Hz), and thus likely also included other nonpersistent currents that correlated with the *F–I* slope.

In acute spinal rats, the Na PICs are usually too small to produce an outright NSR in the *I–V* relation, so Na PICs do not activate in an all-or-nothing manner (no Na plateau produced), unlike the usual case in chronic spinal rats (Li et al. 2004a) or in normal motoneurons treated with 5-HT (Harvey et al. 2005b). Thus in acute spinal rats, once firing is initiated, it can easily be stopped by decreasing the excitation from current injection. That is, once firing slows sufficiently during decreasing current injection (triangular current injection), the upswing of the AHP and the weak depolarization from the Na PIC are not sufficient to overcome the decreasing excitation, so the minimum rate of change of potential (dV/dt) for spike initiation is not reached. At this point firing stops, and this is sometimes at a current greater than that required to recruit the motoneuron ($\Delta I < 0$; i.e., late spike frequency adaptation occurs, see Bennett et al. 2001).

Spinal shock after injury and impact on acute slice preparations

In summary, compared with motoneurons of chronic spinal rats or normal motoneurons treated with 5-HT (Harvey et al. 2005b), greater excitation is required to recruit motoneurons after acute spinal transection because they rest further from threshold, they have lower input resistance, and they have less Ca and Na PICs to help bring the membrane to threshold. Also, if firing is initiated, it does not always continue, especially at low rates, because of the weak Na PICs. Together, these factors play a major role in determining the reduced motoneuron excitability after acute spinal cord injury, and ultimately this helps explain the spinal shock state seen clinically after injury. The reduced excitability seen in acute injury, can be increased by monoamine antagonists (Harvey et al. 2005a) or overcome with monoamine agonists (Harvey et al. 2005b). Thus the massive loss of brain stem–derived monoamines plays a central role in spinal shock after acute injury.

Most of what we know about “normal” motoneurons derives from acute slice preparations (turtle, guinea pig, mouse, etc.), which also suffer from the same massive loss of brain stem monoamines as do acute spinal animals. Thus the firing behavior of motoneurons in these slice preparations is compromised. The motoneurons of chronic spinal rats are much closer to normal because they have PICs more comparable with the brain stem–intact animal (Lee and Heckman 1998a) and have had months to compensate for the loss of monoamines by

increasing sensitivity of receptor pathways that facilitate the PICs (Harvey et al. 2005a,b). Motoneurons of chronic spinal rats do, however, have a significant reduction in dendritic size, compared with normal (e.g., Kitzman 2005), and it remains to be determined whether this influences the function of the motoneuron.

Acknowledgments

We thank L. Sanelli for expert technical assistance and J. Kowalczewski and G. Braybrook for assisting with electron micrographs of electrodes.

GRANTS

This work was funded by National Institute of Neurological Disorders and Stroke Grant RO1 NS-47567-01, the Natural Sciences and Engineering Research Council, Canadian Foundation for Innovation, the Canadian Institutes of Health Research, and the Alberta Heritage Foundation for Medical Research.

References

Alaburda A, Hounsgaard J. Metabotropic modulation of motoneurons by scratch-like spinal network activity. J Neurosci. 2003; 23:8625–8629. [PubMed: 14507961]

Alvarez FJ, Pearson JC, Harrington D, Dewey D, Torbeck L, Fyffe RE. Distribution of 5-hydroxytryptamine-immunoreactive boutons on alpha-motoneurons in the lumbar spinal cord of adult cats. J Comp Neurol. 1998; 393:69–83. [PubMed: 9520102]

Alzheimer C, Schwindt PC, Crill WE. Modal gating of Na^+ channels as a mechanism of persistent Na^+ current in pyramidal neurons from rat and cat sensorimotor cortex. J Neurosci. 1993; 13:660–673. [PubMed: 8381170]

Bennett DJ, Gorassini M, Fouad K, Sanelli L, Han Y, Cheng J. Spasticity in rats with sacral spinal cord injury. J Neurotrauma. 1999; 16:69–84. [PubMed: 9989467]

Bennett DJ, Li Y, Siu M. Plateau potentials in sacrocaudal motoneurons of chronic spinal rats, recorded in vitro. J Neurophysiol. 2001; 86:1955–1971. [PubMed: 11600653]

Bennett DJ, Sanelli L, Cooke C, Harvey PJ, Gorassini MA. Spastic long-lasting reflexes in the awake rat after sacral spinal cord injury. J Neurophysiol. 2004; 91:2247–2258. [PubMed: 15069102]

Cassam AK, Llewellyn-Smith IJ, Weaver LC. Catecholamine enzymes and neuropeptides are expressed in fibres and somata in the intermediate gray matter in chronic spinal rats. Neuroscience. 1997; 78:829–841. [PubMed: 9153661]

Conway BA, Hultborn H, Kiehn O, Mintz I. Plateau potentials in alpha-motoneurones induced by intravenous injection of L-dopa and clonidine in the spinal cat. J Physiol. 1988; 405:369–384. [PubMed: 3255795]

Coraboeuf E. Ionic basis of excitation mechanism in cardiac muscle. Recent Adv Stud Card Struct Metab. 1976; 11:11–18.

Crill WE. Persistent sodium current in mammalian central neurons. Annu Rev Physiol. 1996; 58:349–362. [PubMed: 8815799]

Deisz RA, Fortin G, Zieglgansberger W. Voltage dependence of excitatory postsynaptic potentials of rat neocortical neurons. J Neurophysiol. 1991; 65:371–382. [PubMed: 1826741]

Delgado-Lezama R, Perrier JF, Nedergaard S, Svirskis G, Hounsgaard J. Metabotropic synaptic regulation of intrinsic response properties of turtle spinal motoneurones. J Physiol. 1997; 504:97–102. [PubMed: 9350621]

Eken T, Hultborn H, Kiehn O. Possible functions of transmitter-controlled plateau potentials in alpha motoneurones. Prog Brain Res. 1989; 80:257–267. [PubMed: 2699366]

Fedirchuk B, Dai Y. Monoamines increase the excitability of spinal neurones in the neonatal rat by hyperpolarizing the threshold for action potential production. J Physiol. 2004; 557:355–361. [PubMed: 15090607]

French CR, Sah P, Buckett KJ, Gage PW. A voltage-dependent persistent sodium current in mammalian hippocampal neurons. J Gen Physiol. 1990; 95:1139–1157. [PubMed: 2374000]

Geijo-Barrientos E, Pastore C. The effects of dopamine on the sub-threshold electrophysiological responses of rat prefrontal cortex neurons in vitro. Eur J Neurosci. 1995; 7:358–366. [PubMed: 7773435]

Gorassini MA, Bennett DJ, Yang JF. Self-sustained firing of human motor units. Neurosci Lett. 1998; 247:13–16. [PubMed: 9637398]

Granit R, Henatsch HD, Steg G. Tonic and phasic ventral horn cells differentiated by post-tetanic potentiation in cat extensors. Acta Physiol Scand. 1956; 37:114–126. [PubMed: 13361891]

Guertin PA, Hounsgaard J. Non-volatile general anaesthetics reduce spinal activity by suppressing plateau potentials. Neuroscience. 1999; 88:353–358. [PubMed: 10197758]

Harvey PJ, Li X, Li Y, Bennett DJ. 5-HT_2 receptor activation facilitates a persistent sodium current and repetitive firing in spinal motoneurons of rats with and without chronic spinal cord injury. J Neurophysiol. 2006a; 96:1158–1170. [PubMed: 16707714]

Harvey PJ, Li X, Li Y, Bennett DJ. Endogenous monoamine receptor activation is essential for enabling persistent sodium currents and repetitive firing in rat spinal motoneurons. J Neurophysiol. 2006b; 96:1171–1186. [PubMed: 16760346]

Hounsgaard J, Hultborn H, Jespersen B, Kiehn O. Bistability of alpha-motoneurones in the decerebrate cat and in the acute spinal cat after intravenous 5-hydroxytryptophan. J Physiol. 1988a; 405:345–367. [PubMed: 3267153]

Hounsgaard J, Kiehn O. Serotonin-induced bistability of turtle motoneurones caused by a nifedipine-sensitive calcium plateau potential. J Physiol. 1989; 414:265–282. [PubMed: 2607432]

Hounsgaard J, Kiehn O, Mintz I. Response properties of motoneurones in a slice preparation of the turtle spinal cord. J Physiol. 1988b; 398:575–589. [PubMed: 2455803]

Hsiao CF, Del Negro CA, Trueblood PR, Chandler SH. Ionic basis for serotonin-induced bistable membrane properties in guinea pig trigeminal motoneurons. J Neurophysiol. 1998; 79:2847–2856. [PubMed: 9636091]

Hultborn H, Kiehn O. Neuromodulation of vertebrate motor neuron membrane properties. Curr Opin Neurobiol. 1992; 2:770–775. [PubMed: 1282406]

Kiehn O, Eken T. Prolonged firing in motor units: evidence of plateau potentials in human motoneurons? J Neurophysiol. 1997; 78:3061–3068. [PubMed: 9405525]

Kiehn O, Harris-Warrick RM. Serotonergic stretch receptors induce plateau properties in a crustacean motor neuron by a dual-conductance mechanism. J Neurophysiol. 1992; 68:485–495. [PubMed: 1527571]

Kitzman P. Alteration in axial motoneuronal morphology in the spinal cord injured spastic rat. Exp Neurol. 2005; 192:100–108. [PubMed: 15698623]

Kuo JJ, Schonewille M, Siddique T, Schults AN, Fu R, Bar PR, Anelli R, Heckman CJ, Kroese AB. Hyperexcitability of cultured spinal motoneurons from presymptomatic ALS mice. J Neurophysiol. 2004; 91:571–575. [PubMed: 14523070]

Lee RH, Heckman CJ. Bistability in spinal motoneurons in vivo: systematic variations in persistent inward currents. J Neurophysiol. 1998a; 80:583–593. [PubMed: 9705452]

Lee RH, Heckman CJ. Bistability in spinal motoneurons in vivo: systematic variations in rhythmic firing patterns. J Neurophysiol. 1998b; 80:572–582. [PubMed: 9705451]

Lee RH, Heckman CJ. Enhancement of bistability in spinal motoneurons in vivo by the noradrenergic alpha1 agonist methoxamine. J Neurophysiol. 1999; 81:2164–2174. [PubMed: 10322057]

Lee RH, Heckman CJ. Essential role of a fast persistent inward current in action potential initiation and control of rhythmic firing. J Neurophysiol. 2001; 85:472–475. [PubMed: 11152749]

Li Y, Bennett DJ. Persistent sodium and calcium currents cause plateau potentials in motoneurons of chronic spinal rats. J Neurophysiol. 2003; 90:857–869. [PubMed: 12724367]

Li Y, Gorassini MA, Bennett DJ. Role of persistent sodium and calcium currents in motoneuron firing and spasticity in chronic spinal rats. J Neurophysiol. 2004a; 91:767–783. [PubMed: 14762149]

Li Y, Harvey PJ, Li X, Bennett DJ. Spastic long-lasting reflexes in the chronic spinal rat, studied in vitro. J Neurophysiol. 2004b; 91:2236–2246. [PubMed: 15069101]

Li Y, Li X, Harvey PJ, Bennett DJ. Effects of baclofen on spinal reflexes and persistent inward currents in motoneurons of chronic spinal rats with spasticity. J Neurophysiol. 2004c; 92:2694–2703. [PubMed: 15486423]

Newton BW, Hamill RW. The morphology and distribution of rat serotoninergic intraspinal neurons: an immunohistochemical study. Brain Res Bull. 1988; 20:349–360. [PubMed: 3365563]

Nishimura Y, Schwindt PC, Crill WE. Electrical properties of facial motoneurons in brainstem slices from guinea pig. Brain Res. 1989; 502:127–142. [PubMed: 2819451]

Perrier JF, Hounsgaard J. 5-HT2 receptors promote plateau potentials in turtle spinal motoneurons by facilitating an L-type calcium current. J Neurophysiol. 2003; 89:954–959. [PubMed: 12574471]

Perrier JF, Mejia-Gervacio S, Hounsgaard J. Facilitation of plateau potentials in turtle motoneurones by a pathway dependent on calcium and calmodulin. J Physiol. 2000; 528:107–113. [PubMed: 11018109]

Powers RK, Binder MD. Effective synaptic current and motoneuron firing rate modulation. J Neurophysiol. 1995; 74:793–801. [PubMed: 7472383]

Powers RK, Binder MD. Persistent sodium and calcium currents in rat hypoglossal motoneurons. J Neurophysiol. 2003; 89:615–624. [PubMed: 12522206]

Prather JF, Powers RK, Cope TC. Amplification and linear summation of synaptic effects on motoneuron firing rate. J Neurophysiol. 2001; 85:43–53. [PubMed: 11152704]

Schlue WR, Richter DW, Mauritz KH, Nacimiento AC. Responses of cat spinal motoneuron somata and axons to linearly rising currents. J Neurophysiol. 1974; 37:303–309. [PubMed: 4815207]

Schmidt BJ, Jordan LM. The role of serotonin in reflex modulation and locomotor rhythm production in the mammalian spinal cord. Brain Res Bull. 2000; 53:689–710. [PubMed: 11165804]

Schroder HD, Skagerberg G. Catecholamine innervation of the caudal spinal cord in the rat. J Comp Neurol. 1985; 242:358–368. [PubMed: 4086667]

Schwindt PC, Crill WE. Factors influencing motoneuron rhythmic firing: results from a voltage-clamp study. J Neurophysiol. 1982; 48:875–890. [PubMed: 7143033]

Stafstrom CE, Schwindt PC, Chubb MC, Crill WE. Properties of persistent sodium conductance and calcium conductance of layer V neurons from cat sensorimotor cortex in vitro. J Neurophysiol. 1985; 53:153–170. [PubMed: 2579215]

Taddese A, Bean BP. Subthreshold sodium current from rapidly inactivating sodium channels drives spontaneous firing of tuberomammillary neurons. Neuron. 2002; 33:587–600. [PubMed: 11856532]

Urbani A, Belluzzi O. Riluzole inhibits the persistent sodium current in mammalian CNS neurons. Eur J Neurosci. 2000; 12:3567–3574. [PubMed: 11029626]

White SR, Fung SJ. Serotonin depolarizes cat spinal motoneurons in situ and decreases motoneuron afterhyperpolarizing potentials. Brain Res. 1989; 502:205–213. [PubMed: 2819461]

Xu W, Lipscombe D. Neuronal Ca(V)1.3alpha(1) L-type channels activate at relatively hyperpolarized membrane potentials and are incompletely inhibited by dihydropyridines. J Neurosci. 2001; 21:5944–5951. [PubMed: 11487617]

Zeng J, Powers RK, Newkirk G, Yonkers M, Binder MD. Contribution of persistent sodium currents to spike-frequency adaptation in rat hypoglossal motoneurons. J Neurophysiol. 2005; 93:1035–1041. [PubMed: 15356185]

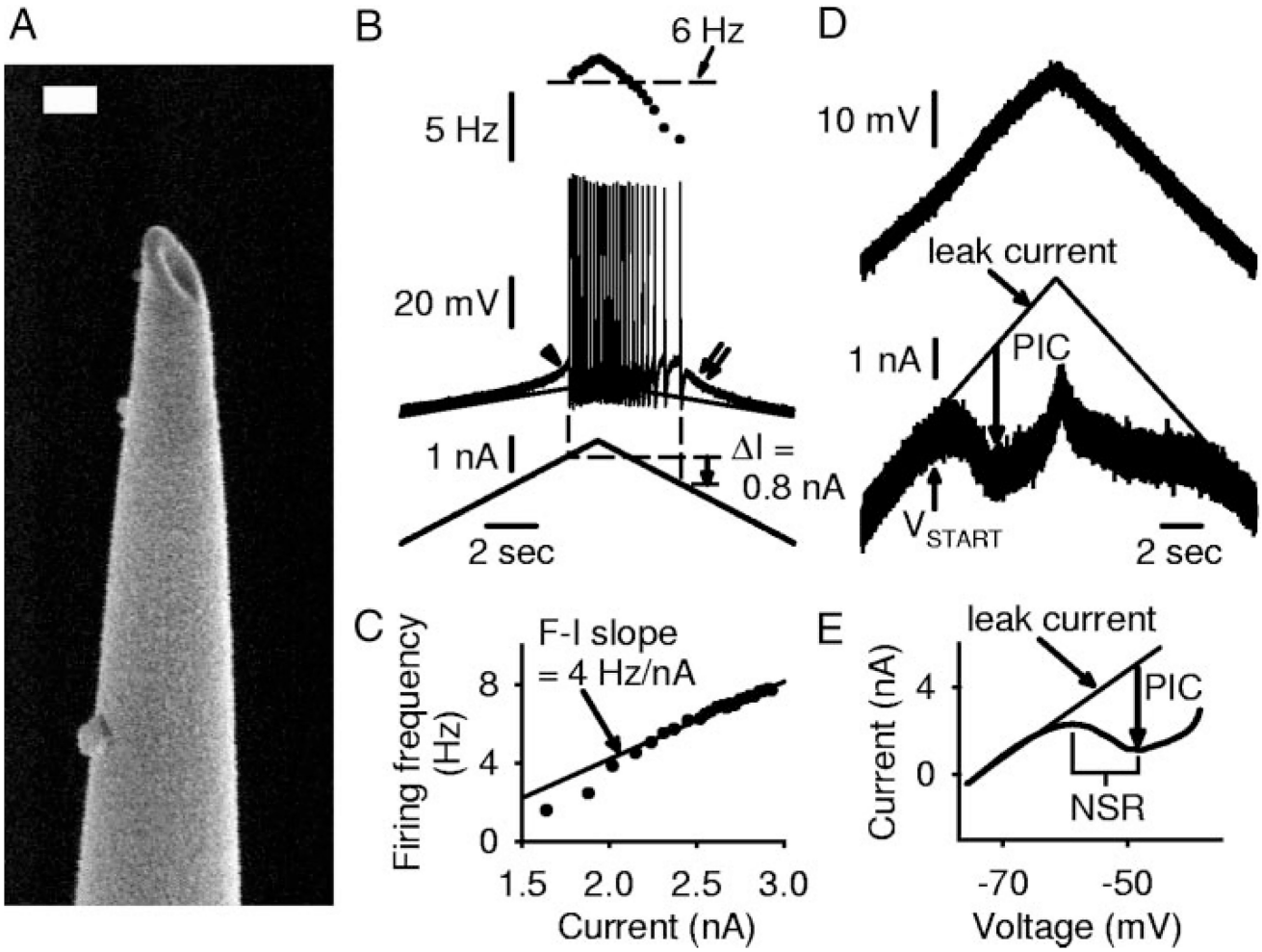

FIG. 1.

Intracellular motoneuron recording methods for rat in vitro sacrocaudal cord. *A*: electron microscope image of a bevelled intracellular electrode tip. Electrode was bevelled by holding the tip against a rotating stone (at 22°), while continuously monitoring its resistance with saline on the stone, until the resistance dropped to 25–30 MΩ. Scale bar = 200 nm. *B*: intracellular recording in discontinuous current clamp (DCC) mode of motoneuron from a chronic spinal rat. *Bottom*: slow triangular current ramp (0.4 nA/s). *Middle*: membrane potential with repetitive firing, showing extrapolated leak potential (thin line). Note subthreshold acceleration (arrowhead), self-sustained firing (positive $\Delta I = 0.8$ nA; dashed lines, onset and offset of firing), and afterpotential (double arrow). *Top*: firing frequency (horizontal line indicates 6 Hz). Note hysteresis in firing frequency. *C*: instantaneous firing frequency (*F*) from triangular current ramp in *B*, plotted against current (*I*). *F–I* slope measured by regression analysis of linear region of *F–I* plot was 4 Hz/nA in this cell. *D*: same motoneuron as *B*, during slow triangular voltage ramp from −80 to −40 mV and back to −80 mV (3.5 nA/s; *top*) in single-electrode voltage clamp (SEVC) mode. At persistent inward current (PIC) onset (VSTART), current (*bottom*) deviated from the extrapolated leak current (thin line). PIC amplitude estimated from maximum difference between leak current

and actual current, shown with downward arrow. *E*: same data as *D*, with current filtered and plotted against voltage (*I*–*V* plot). Note negative-slope region (NSR) in *I*–*V* relation.

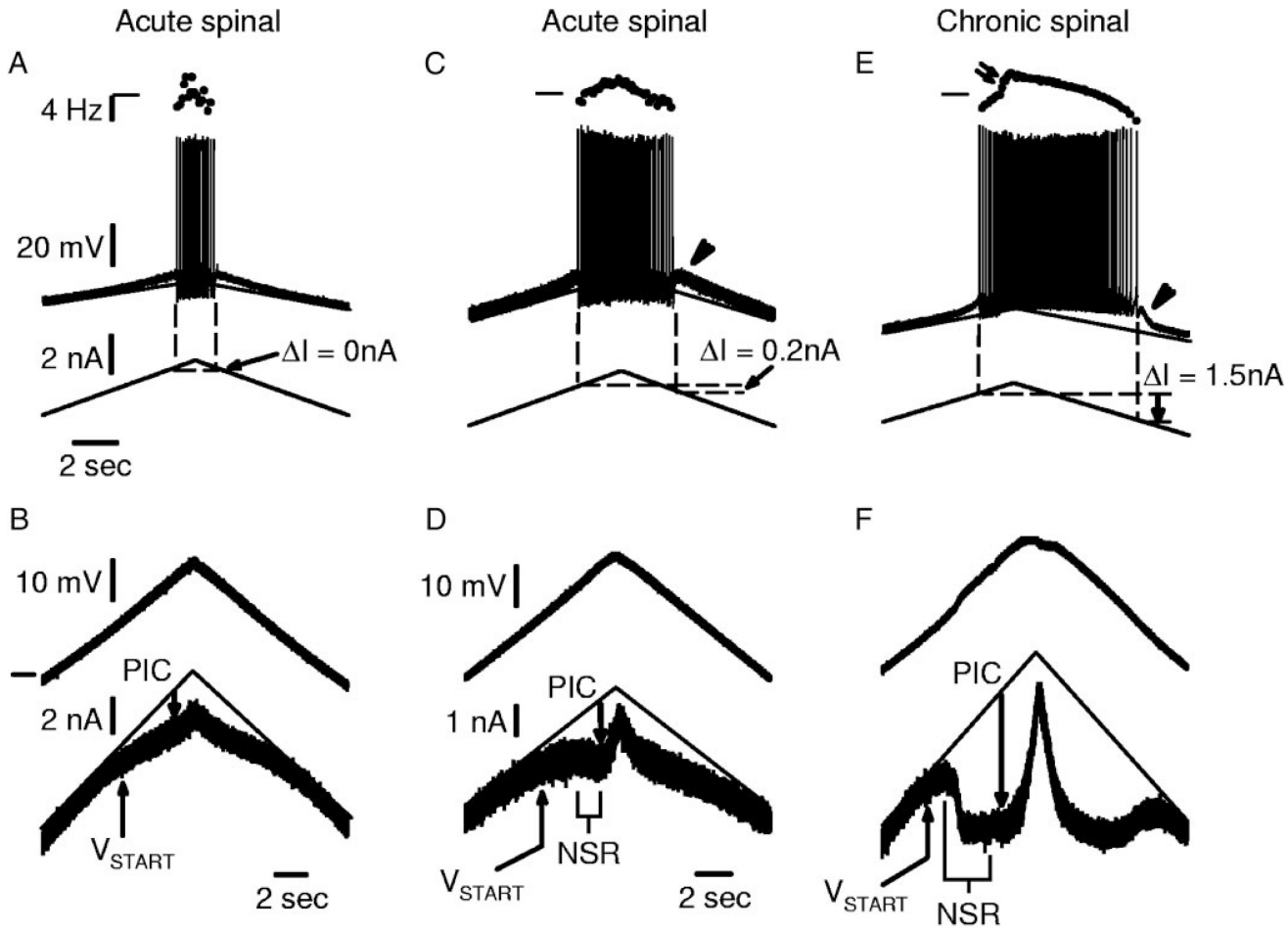

FIG. 2.

Motoneurons from acute spinal rats have small PICs. *A*: recording of a motoneuron in acute spinal rat that did not exhibit any self-sustained firing during a triangular current ramp (ΔI= 0 nA). *B*: voltage-clamp recording from same cell with slow voltage ramp starting at −80 mV (horizontal mark). Note small PIC that induces an inflection (flattening) in current response. *C*: different motoneuron from acute spinal rat with small subthreshold acceleration in membrane potential before the 1st spike and small afterdepolarization after cessation of firing (arrowhead). Firing frequency increased linearly with current, and there was a small amount of self-sustained firing (ΔI> 0 nA; see METHODS). *D*: voltage ramps for cell in *C* showing PIC inducing a small NSR associated with self-sustained firing ability. *E*: motoneuron from chronic spinal rat showing much greater self-sustained firing (greater ΔI), and nonlinearity (acceleration) in firing frequency induced by Ca PIC onset (double arrow). *F*: large PICs and NSR associated with self-sustained firing in *E*. Scale bars in *A* apply to *C* and *E*. Scale bars in *D* also apply to *F*.

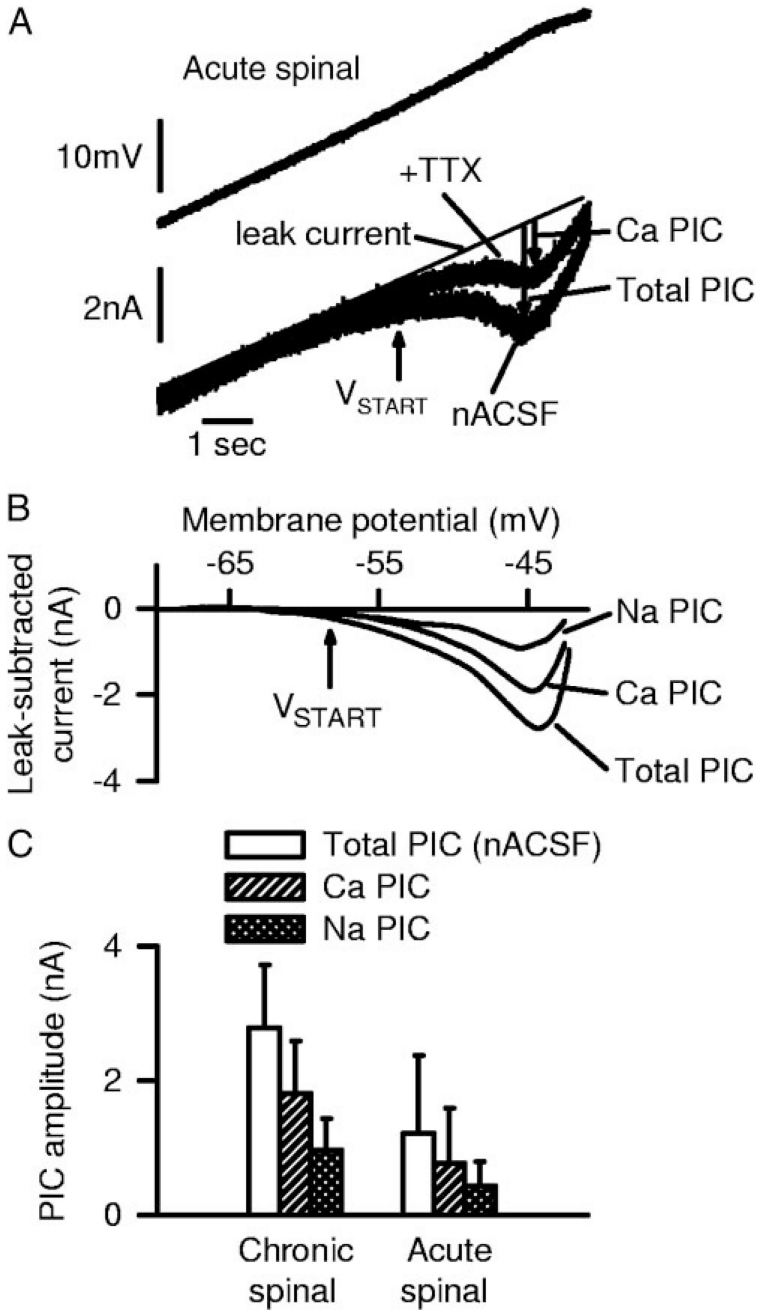

FIG. 3.

TTX-sensitive Na PICs and TTX-resistant Ca PICs in motoneurons of acute spinal rats. *A*: current response to voltage ramp before and after TTX application, with leak current shown with thin line (as in upward ramp of Fig. 2*D*). PICs indicated by downward arrows. Notice reduction in PIC with TTX, leaving only a TTX-resistant PIC (Ca PIC). *B*: filtered data from *A* with the leak current (thin line in *A*) subtracted (leak-subtracted current), and plotted against voltage. Trace labeled total PIC is the leak-subtracted current in normal artificial cerebrospinal fluid (nACSF), and trace labeled Ca PIC is the leak-subtracted TTX-resistant current in *A*, which is Cd^{2+} -sensitive (data not shown). Trace labeled Na PIC is difference

between total PIC and Ca PIC (TTX-sensitive PIC). *C*: averages of total PIC, Na PIC, and Ca PIC peak amplitudes from all acute and chronic spinal rats tested with TTX, each significantly larger in chronic spinal rats.

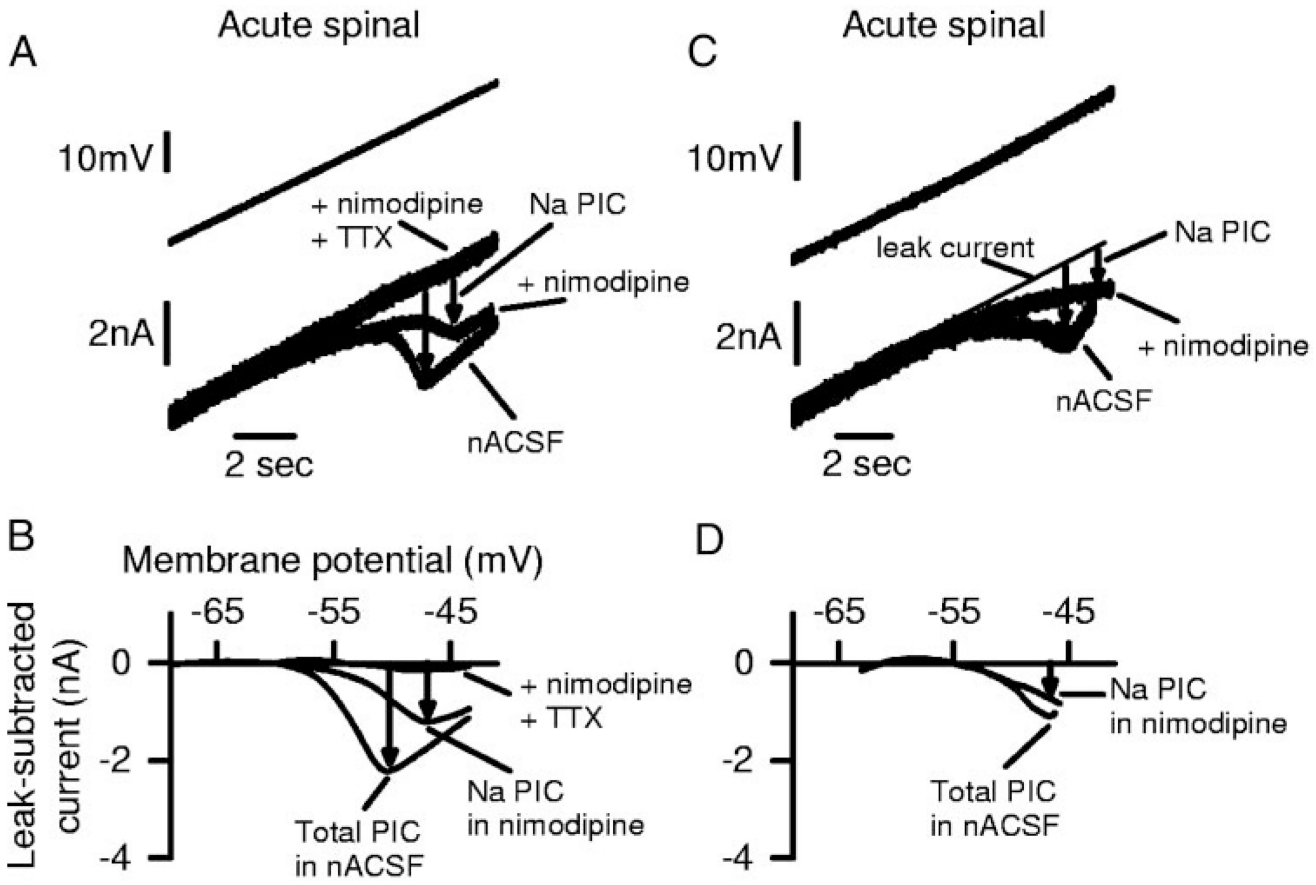

FIG. 4.

Ca PIC is blocked by nimodipine, leaving only a TTX-sensitive Na PIC in motoneurons from acute spinal rats. *A*: same format as Fig. 3*A*, but with 15 μM nimodipine added 1st to block L-type calcium channels mediating the Ca PIC. Downward arrows indicate amplitude of total PIC before nimodipine (*left*) and Na PIC in nimodipine (*right*). Addition of TTX blocked Na PIC, leaving linear current response. *B*: filtered and leak-subtracted currents from *A*, plotted against voltage (*I–V* plots, as in Fig. 3*B*), showing total PIC in nACSF, Na PIC in nimodipine, and block of all PICs in nimodipine and TTX. *C* and *D*: same format as *A* and *B*, but from different acute spinal rat motoneuron with smaller, more typical Na PIC remaining in nimodipine. TTX was not added in this motoneuron.

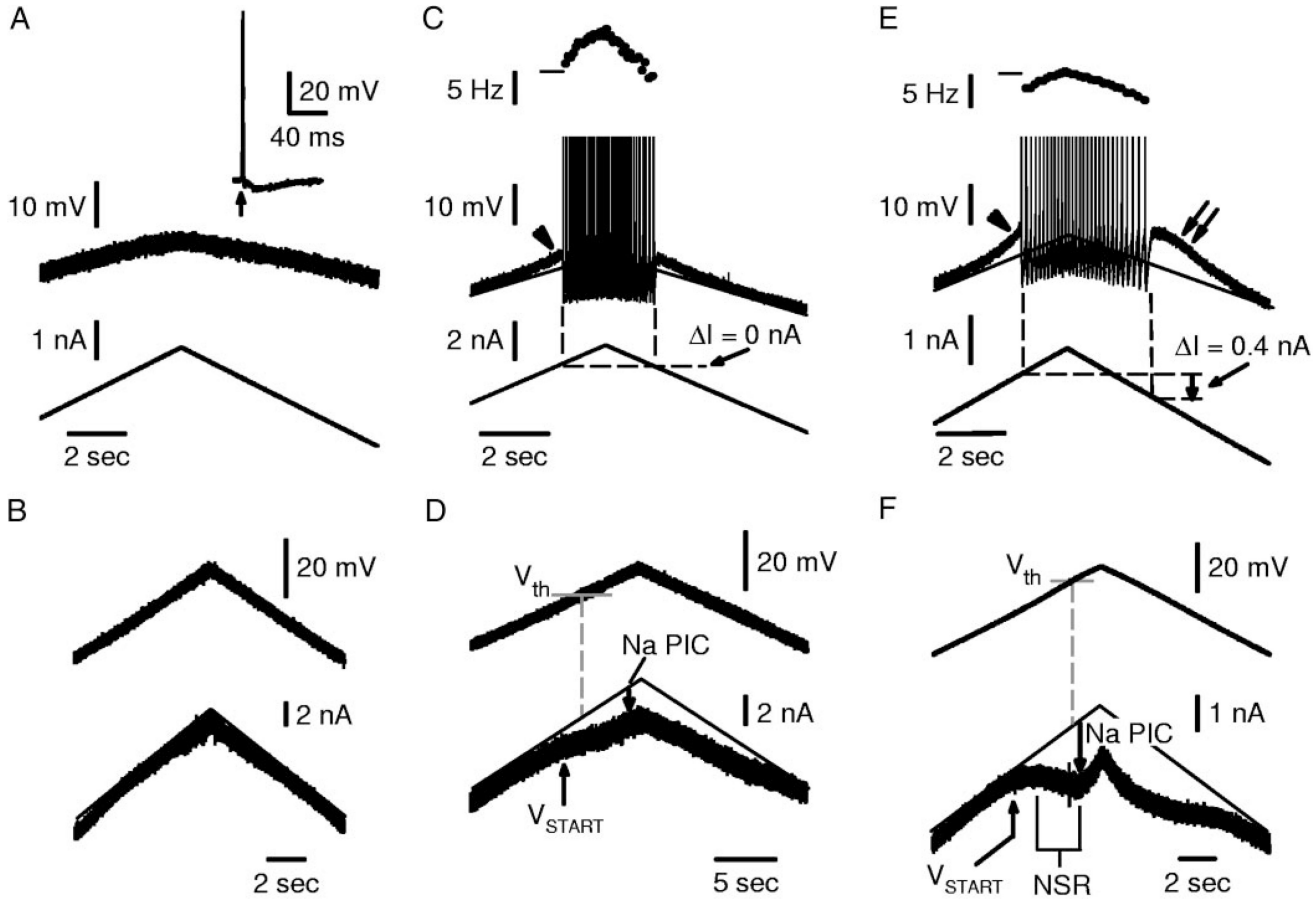

FIG. 5.

Variability in repetitive firing ability is related to Na PIC amplitude. All recordings (*A*–*F*) are from motoneurons of acute spinal rats with 15 μM nimodipine present to block Ca PICs (same format as Fig. 2). *A*: motoneuron that was unable to initiate repetitive firing with standard slow current ramps, although it had a full-height spike (*inset*) in response to antidromic stimulation (up arrow). *B*: motoneurons with poor firing ability, as in *A*, lacked Na PICs (linear current response to voltage ramp; same cell as in *A*). *C*: typical motoneuron for acute spinal rats, with small subthreshold acceleration (arrowhead) and repetitive firing (top of spikes clipped), but no self-sustained firing ($\Delta I = 0$ nA). *D*: these typical motoneurons had small Na PICs that only caused a flattening in the current response to a voltage ramp and no NSR. Note that V_{START} occurs below firing level (V_{th}). *E*: extreme motoneuron that had self-sustained firing ($\Delta I > 0$ nA) and relatively low minimum firing rate (<6 Hz). Note large subthreshold acceleration (arrowhead) and after-potential (double arrow), indicating underlying Na plateau. *F*: same motoneuron as in *E* had a Na PIC large enough to induce an NSR. Horizontal marks at left of frequency plots indicate 10 Hz.

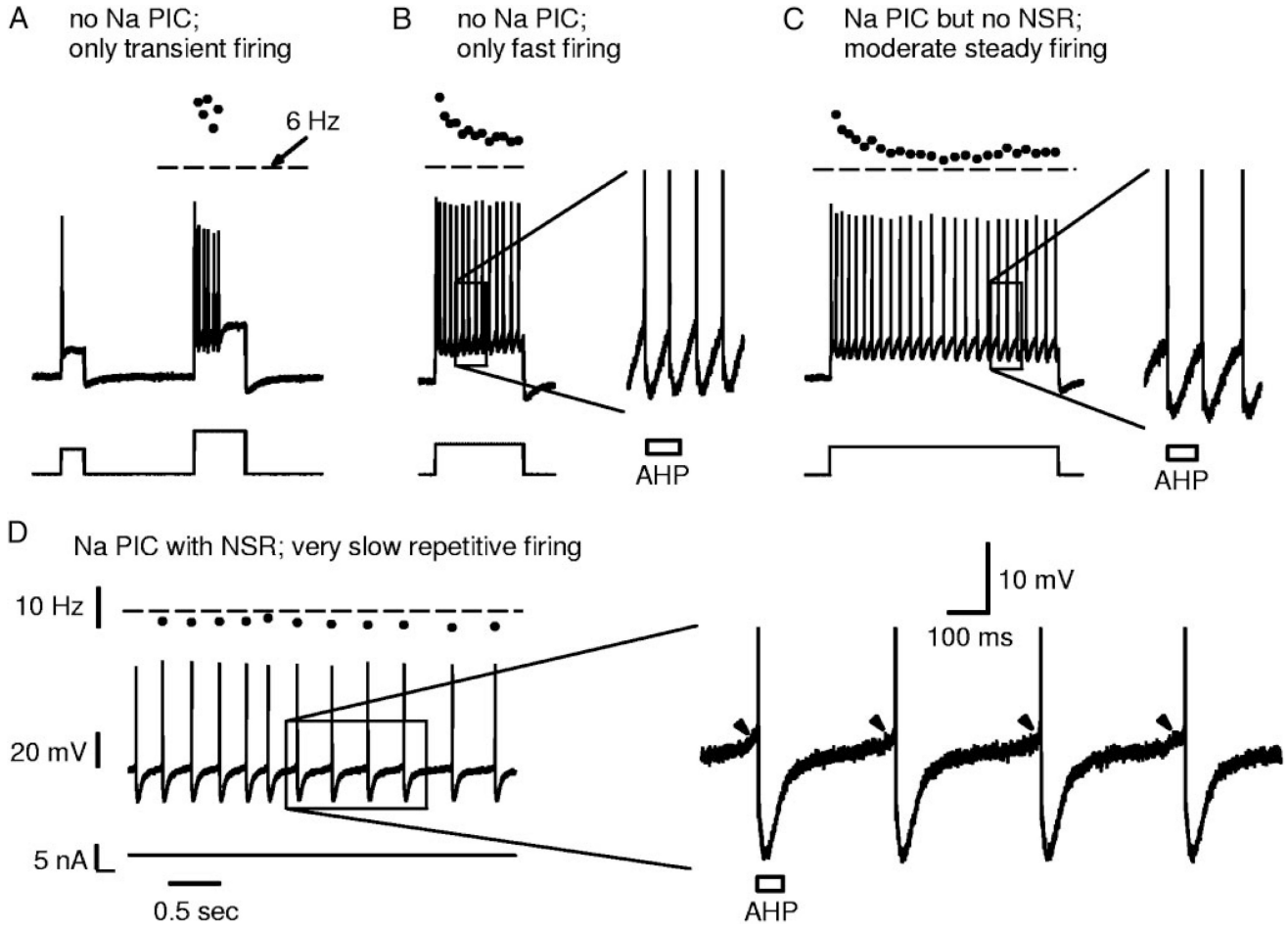

FIG. 6.

Na PIC amplitude controls firing ability near threshold. All traces recorded in current clamp, with depolarizing steps from rest in acute spinal rat motoneurons in nimodipine (Ca PIC blocked). *A*: example motoneuron with no Na PIC (as in Fig. 5*B*), where only transient firing occurred with depolarizing steps at threshold (*left*) or above threshold (*right*). *B*: different motoneuron with no Na PIC; repetitive firing occurred with large step pulses in this cell, but only at high rates (≫6 Hz), whereas firing was only transient with smaller current steps, like in *A* (data not shown). *Inset* in *B* is close-up on a few spikes. Note that interspike interval is shorter than AHP duration (indicated by box). *C*: motoneuron with a small Na PIC but no negative-slope region (as in Fig. 5*D*); in this cell repetitive firing occurred near threshold, and the maximum interspike interval was roughly equal to the AHP duration (*inset*). *D*: motoneuron with large Na PIC and NSR (as in Fig. 5*F*); in this cell, slow steady firing below 6 Hz (horizontal dashed line) was produced when the cell was held near threshold. Note interspike interval much longer than AHP duration (*inset*), and fast acceleration in membrane potential just prior to each spike (arrowheads). Horizontal mark in current scale bar in *D* indicates 0 nA. All figures and insets to same scale shown in *D*.

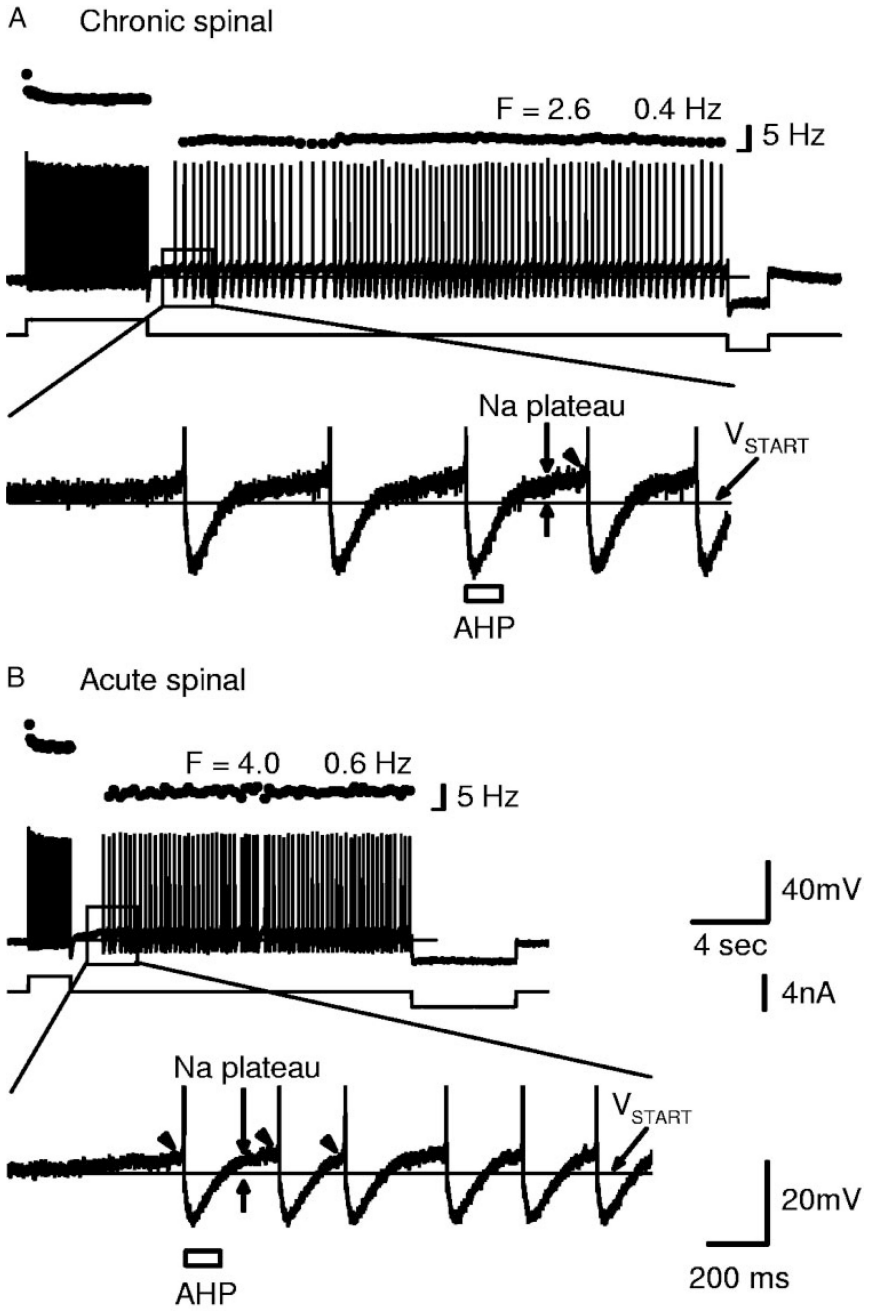

FIG. 7.

Motoneurons of acute spinal rats, with large enough Na PICs to produce an NSR, exhibited steady very slow firing similar to that commonly seen in chronic spinal rats. *A*: *top*: current clamp recording of chronic spinal rat motoneuron held near threshold (in nimodipine). Brief depolarizing current pulse initiated a Na plateau and self-sustained firing at very low average frequency (2.6 ± 0.4 Hz), terminated by a hyperpolarizing current pulse (*right*). *Bottom*: amplification of *top* showing long interspike intervals (longer than AHP). Note that the Na PIC was activated before each spike (Na plateau above V_{START}, fast acceleration at arrowhead), but the AHP dropped the membrane potential below V_{START}, which deactivated

the Na PIC/plateau. *B*: *top*: motoneuron from acute spinal rat (in nimodipine) that had Na PIC large enough to produce an NSR, also had steady slow firing mediated by Na plateaus as in *A*. *Bottom*: steady repetitive firing at frequencies below 6 Hz, with interspike intervals again greatly exceeding the AHP duration (determined from antidromic stimulation at rest). Again, note activation of Na plateau (vertical arrows) and fast acceleration (arrowhead) before spike. Scale bars in *B* also apply to *A*. Horizontal mark at bottom of frequency scale bars indicates 0 Hz.

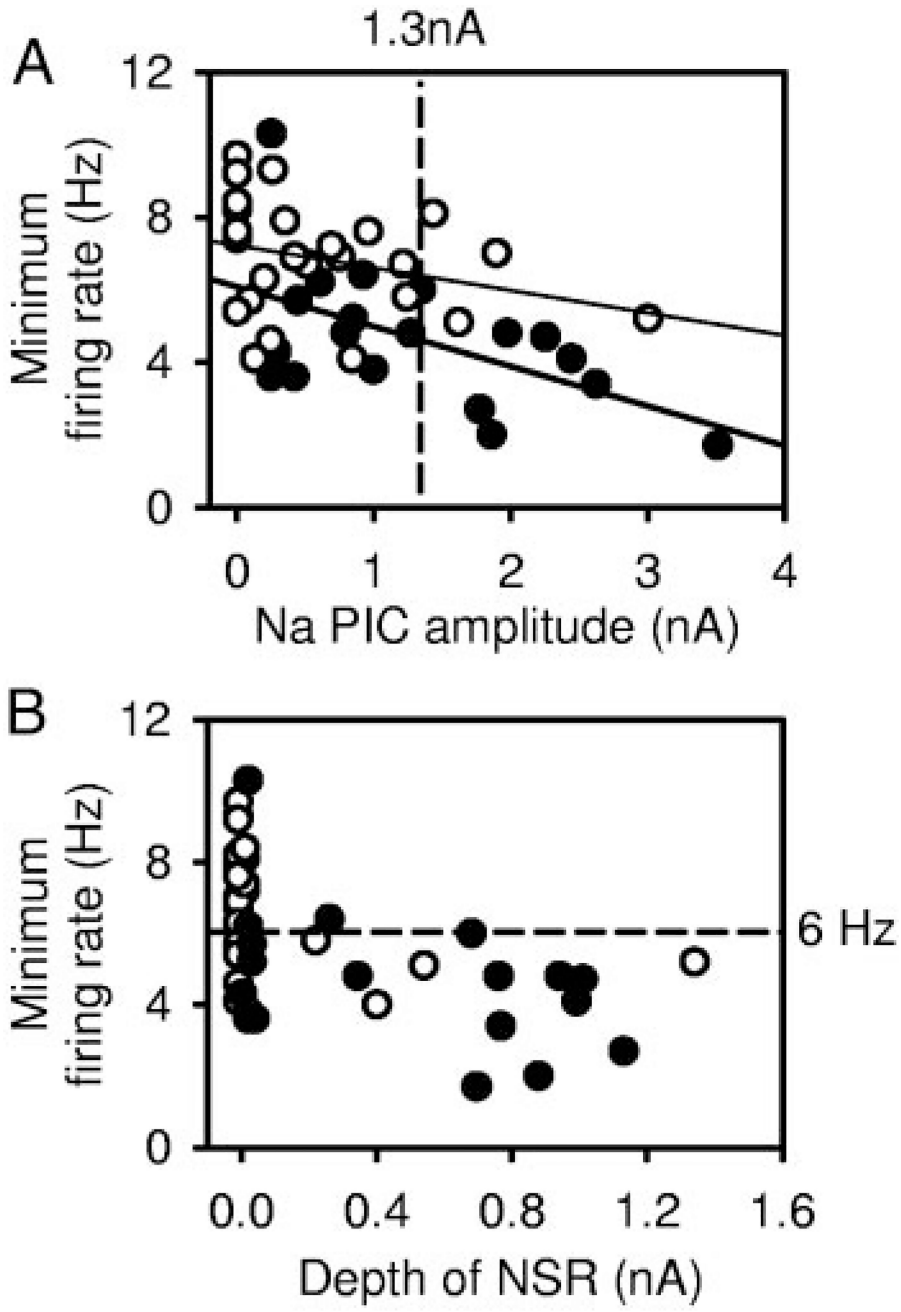

FIG. 8.

Na PIC amplitude correlates with minimum firing rate. *A*: in chronic spinal rat motoneurons (●, thick regression line), large Na PICs correlated significantly with low minimum firing rates (r= 0.538). Acute spinal rat motoneurons (○, thin regression line) also had a trend toward Na PICs correlating with minimum firing rates, but this was not significant. *B*: motoneurons with an NSR in current trace were more likely to exhibit steady slow firing (<6 Hz, below horizontal dashed line). The 4 acute spinal rat motoneurons with an NSR (>25CB; at *right*) had minimum firing rates at the low end of range for normal motoneurons.

With chronic spinal injury, many more motoneurons had an NSR in current trace and these had an average minimum firing rate below 6 Hz.

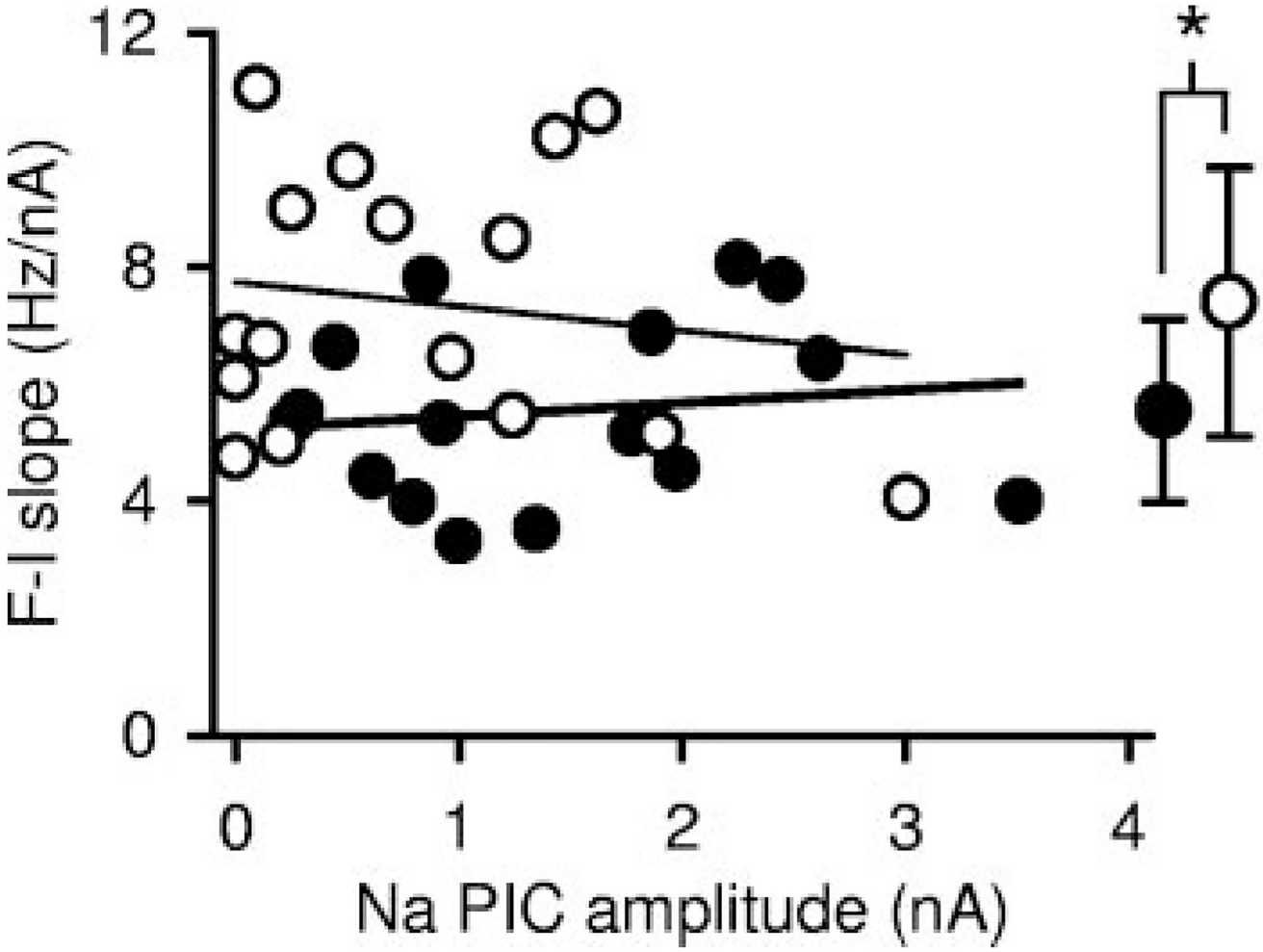

FIG. 9.

F–I slope is not related to the Na PIC amplitude. *F–I* slope measured from response to slow current ramps in the presence of nimodipine (Ca PIC blocked) in motoneurons from acute spinal (○, thin regression line) and chronic spinal (●, thick regression line) rats, and plotted against Na PIC amplitude. No significant correlation was observed between *F–I* slope and Na PIC amplitude in either group. Average *F–I* slopes plotted at *right* show that motoneurons of acute spinal rats had significantly higher *F–I* slopes than motoneurons of chronic spinal rats.

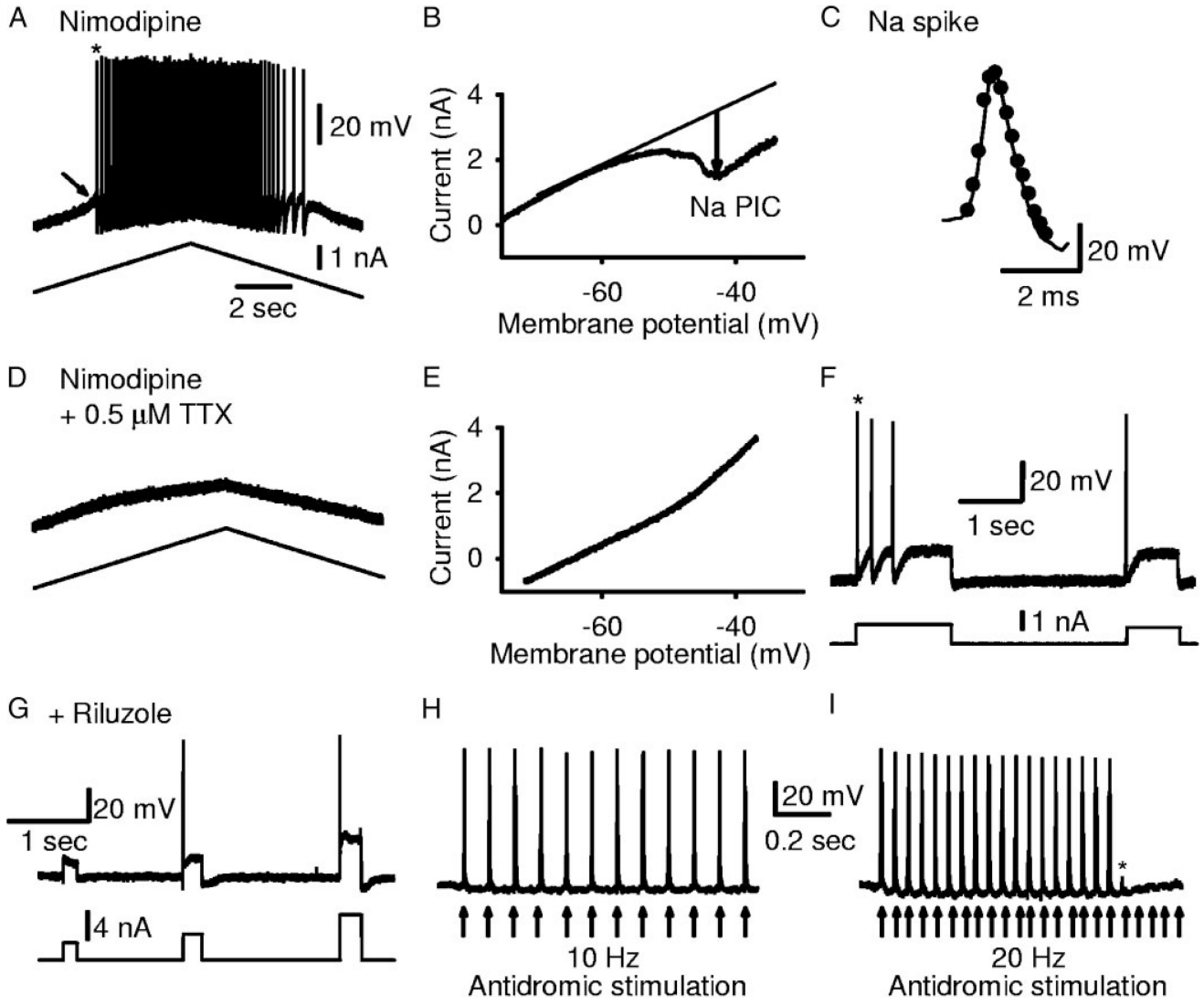

FIG. 10.

Selectively blocking the Na PIC eliminates repetitive firing but not the fast sodium spike. *A*: motoneuron from chronic spinal rat recorded in nimodipine showing typical repetitive firing during slow current ramps. *B*: current-voltage plot response to slow voltage ramp in nimodipine, for same cell as in *A*. Note the clear NSR and large Na PIC (downward arrow). *C*: overlay of the 1st spike from current ramp in nimodipine (thin line, from *A*) with the 1st spike from current step in nimodipine plus low-dose TTX (dots; from spike in *F*). *D*: application of low-dose TTX (0.5 µM) to the cell in *A* and *B* (with nimodipine present) eliminated all repetitive firing ability during slow current ramps, even though the fast sodium spike was not blocked (*C* and *F*). *E*: Na PIC was blocked by low-dose TTX, when lack of firing in *D* was recorded. *F*: in low-dose TTX, current steps still elicited 1–3 spikes, indicating transient sodium currents were not blocked. *G*: another motoneuron with riluzole (20 µM), rather than TTX, used to block the Na PIC (PIC not shown). Again, only transient firing was possible during current steps (*G*) and not ramps (not shown). *H*: with the Na PIC blocked in riluzole, motoneurons could still fire in response to repeated antidromic

stimulation (1 spike for each stimulation at arrow; 10 Hz repetition); thus the spike was still capable of being activated repeatedly. *I*: Same as *H*, but at 20-Hz antidromic stimulation. Spike activation eventually failed (*) with repeated high-frequency stimulation.